Bivalve shell growth from molecular to sclerochronological scale: Environment and intrinsic factors control increment deposition

Victoria Louis, Florian Desbordes, Laurence Besseau, Franck Lartaud

Marine Environmental Research 202 (2024) 106730

Contents lists available at ScienceDirect

Marine Environmental Research

journal homepage: www.elsevier.com/locate/marenvrev

Bivalve shell growth from molecular to sclerochronological scale: Environment and intrinsic factors control increment deposition

Victoria Louis [a,b,*], Florian Desbordes [a], Laurence Besseau [b,1], Franck Lartaud [a,1]

[a] Sorbonne Université, CNRS, Laboratoire d'Ecogéochimie des Environnements Benthiques, LECOB, F-66650, Banyuls-sur-Mer, France
[b] Sorbonne Université, CNRS, Biologie Intégrative des Organismes Marins, BIOM, F-66650, Banyuls-sur-Mer, France

ARTICLE INFO

Keywords:
Biomineralisation genes
Mussel
Mytilus galloprovincialis
Mediterranean environment
Biological clocks
Sclerochronology
Semi-enclosed coastal lagoon

ABSTRACT

Biomineralisation of bivalve shells raises questions at the level of genes to the final calcified product. For the first time, gene expression has been studied in association with growth increment deposition in the mussel *Mytilus galloprovincialis*. A short-term experiment highlighted that biomineralisation genes exhibit a rhythm of expression consistent with the observed tidal increment formation. Long-term mark-recapture experiments were conducted in three Mediterranean environments and revealed that the mussel shells harbour complex incrementation regimes, consisting of daily, tidal and a mixed periodicity of ~1.7 growth increment.d^{-1} formed. The latter is likely related to the local tidal regime, although the mussels were continuously submerged and exposed to a small tidal range. The pattern of growth increments shifted from mixed to daily in Mediterranean lagoon, and to tidal at sea, probably linked to biological clocks. Based on our results and the literature, a hypothetical model for mussel shell increment formation in various habitats is proposed.

1. Introduction

Bivalve biomineralisation is a dynamic process that shows changes in the rate of deposition and the type of material deposited (Schöne 2008; Louis et al., 2022). This is observed at different levels, from gene expression to the final product, the shell, although these aspects have so far been studied separately (Miyazaki et al., 2008; Schöne 2008; Checa 2018; Louis et al., 2022). Shell growth patterns consist of the alternation of calcified growth increments and organic-rich lines, corresponding to growth slowdowns or breaks (Lutz and Rhoads 1977; Karney et al., 2012). Sclerochronological analyses have shown that bivalve shells contain several periodicities through the formation of increments and their variation in width (i.e. annual, lunar, semi-lunar, lunidian, daily, tidal and below) (Schöne 2008; Louis et al., 2022). Cyclic oscillations of environmental variables seem to be an important component for the dynamics of the increment formation (Witbaard et al., 1998; Schöne et al., 2005b; Rodríguez-Tovar 2014). Therefore, shells are considered as biological archives and can be used to reconstruct (paleo)climatic and (paleo)environmental variations, including seasonal to infra-seasonal scales (Schöne et al., 2005a; de Winter et al., 2020).

Tides are commonly considered to be a predominant factor in the origin of shell increments periodicity, especially in intertidal areas (Lutz and Rhoads 1977). In this type of environment, one growth line and one increment are assumed to represent 12.4 h of growth. At low tide, the valves are closed during emersion, causing a decrease in the internal pH of the organism. This acidification leads to a slight decalcification of the shell. Therefore, at high tide, the biomineralisation process takes place on this layer, forming a layer richer in organic material, the growth line, which is covered by a more calcified part, the increment. While tides are classically considered to be the main driver of the increment formation in habitats with large tidal ranges, few studies have focused on environments where tides are small or absent. Sclerochronological studies of bivalves inhabiting the Mediterranean Sea, an area that is mostly subject to low tidal range, are mainly dedicated to the analysis of the annual increment formation (Peharda et al., 2016; Bargione et al., 2020). However, in the French Mediterranean coastal lagoons, the oyster

* Corresponding author. Sorbonne Université, CNRS, Laboratoire d'Ecogéochimie des Environnements Benthiques, LECOB, F-66650, Banyuls-sur-Mer, France.
E-mail address: victoria.louis96@gmail.com (V. Louis).
[1] Co-last authors.

https://doi.org/10.1016/j.marenvres.2024.106730
Received 24 May 2024; Received in revised form 1 September 2024; Accepted 2 September 2024
Available online 4 September 2024

Magallana gigas and the mussel *Mytilus galloprovincialis* are suggested to form daily increments (Langlet et al., 2006; Andrisoa et al., 2019). Photoperiod and temperature have been proposed as potential drivers. But finally, we still lack knowledge about the precise role of environmental conditions in the formation of shell growth increments for these types of ecosystems where tides may not be as the main environmental variable.

In this study, based on molecular and sclerochronological approaches, we propose an integrated view of the dynamic process of bivalve shell biomineralisation, linking gene expression to shell growth patterns for the first time. We worked on two time scales. At the daily time scale, the expression of genes related to biomineralisation was measured in *M. galloprovincialis* mussels from the bay of Banyuls-sur-Mer, Western Mediterranean Sea, where the tidal range is $\leq$ 30 cm, and compared with the rhythm of growth increments formed during this period. On longer time scale (i.e. 1 year), shell growth patterns of *M. galloprovincialis* from different types of Mediterranean habitats were characterised and compared to the environmental variability. Based on mark-recapture technique, mussels were reared in two Mediterranean coastal lagoons (i.e. Salses-Leucate lagoon and Canet-Saint-Nazaire lagoon) and at sea in the bay of Banyuls-sur-Mer, in the Gulf of Lion, from June 2020 to June 2021. These areas, which have different environmental dynamics, were used (1) to test the maintenance of the growth rhythm of the basal unit, the growth increment, under changing extrinsic conditions, and (2) to identify the main drivers of the periodicity of mussel biomineralisation.

2. Material and methods

2.1. Study sites

Two Mediterranean coastal lagoons and one site at sea from the southern part of the French Mediterranean coast were selected for this study (Fig. 1). The sea site chosen for this study was the bay of Banyuls-sur-Mer (Occitanie, France), where mussels have been seen growing between 1 and 15 m depth, including on the flank of the SOLA buoy, an autonomous station of the Oceanological Observatory of Banyuls-sur-Mer, located in half a nautical mile from the coast (Fig. 1A). This area is monitored as part of the SOMLIT from ILICO national program and the JERICO European research infrastructure.

Mediterranean coastal lagoons are shallow inland water bodies formed 15 kyr BP during the Flandrian transgression, separated from the sea by a sandy barrier interrupted by small inlets, which currently correspond to artificial openings ensuring a permanent connection with

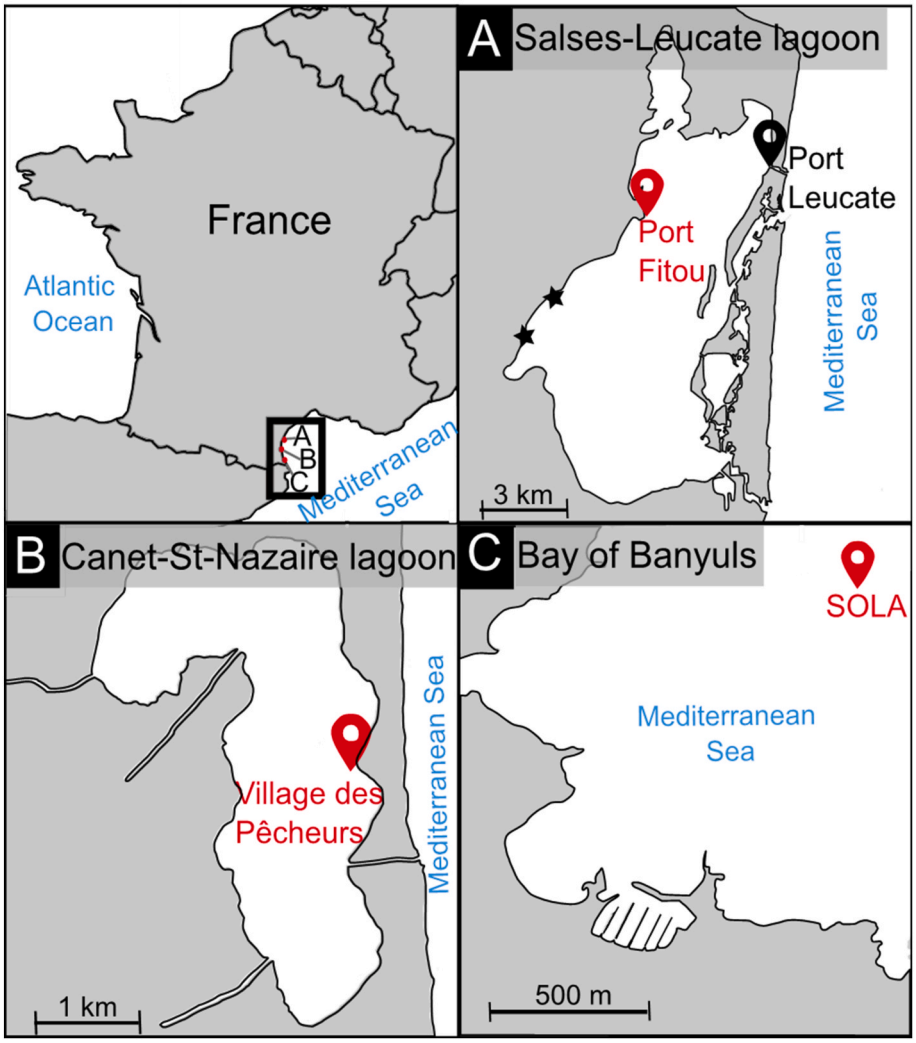

Fig. 1. Locations of the 3 study locations along the southern French Mediterranean coast. (A) In the bay of Banyuls-sur-Mer, mussels were collected and redeployed on the SOLA oceanographic buoy (red sign). (B) The Salses-Leucate lagoon has three main seawater inlets on the eastern side and two main groundwater discharges on the western side (black stars). Mussels were collected near the seawater inlet of Port Leucate (black sign) and transferred to the study site (red sign) located at Port Fitou. (C) The Canet-St-Nazaire lagoon has a main seawater inlet and is supplied in freshwater by three small rivers. Mussels were collected and redeployed in the study point, Village des Pêcheurs (red sign).

the Mediterranean seawater (Arnaud and Raimbault 1969; Pérez-Ruzafa et al., 2019). The Salses-Leucate (SL) lagoon is connected to the sea by three inlets and has a continuous freshwater supply through two main groundwater discharges (Fig. 1B) (Hervé and Bruslé 1980; Bec et al., 2011). This lagoon has an average depth of 2 m, a surface area of 54 km^2 and is oligotrophic (Souchu et al., 2010). It is a shellfish farming site, mainly for oysters. The Canet-Saint-Nazaire (CSN) lagoon is smaller (6 km^2) and shallower (average depth: 0.35 m) (Hervé and Bruslé, 1981; Bec et al., 2011). It has only one seawater inlet and is supplied in freshwater by three small rivers, which are partially obstructed or dry for part of the year (Fig. 1C). The CSN lagoon is considered as hypertrophic and the water quality is poor due to the low water circulation, which causes an increase in the concentrations of nitrogen and phosphate compounds (Derolez et al., 2021; Fiandrino et al., 2021). Moreover, the accumulation of organic matter and sediments can cause low oxygen concentrations (<5 $mg.L^{-1}$) during warm weather. Mediterranean lagoons are known to be highly dynamic environments, responding more quickly to climatic conditions than the open sea (Pérez-Ruzafa et al., 2019).

All areas are subject to a small tidal range ($\leq$30 cm), associated with mixed semidiurnal tides with diurnal inequality. This means that when the tidal coefficient is small, there is a shift from a semidiurnal to a diurnal tidal regime (SHOM 2020).

2.2. Mussel collection and environmental parameters measurement

2.2.1. Short-term in situ experimental design

Ten mussels were collected every 4 h at the SOLA site over a period of 36 h, from midday on September 9, 2020 to midnight on September 11, 2020 (i.e. a total of 100 mussels; Table S.1). The mussels used were subtidal, as were all the mussels used in this study. A piece of the posterior region of the mantle was sampled and flash-frozen in liquid nitrogen for molecular analysis. In parallel, physico-chemical measurements in the water column were carried out by the Banyuls Observation Sea Service (BOSS). Water temperature and salinity were measured using a Sea-bird SBE19-plus CTD probe. Water was sampled using 12 L Niskin bottle. Concentrations of chlorophyll *a* and phaeopigments were measured by filtering 300 mL on Whatman GF/F 25 mm filters. Pigments were extracted with 90% acetone and concentrations were measured by fluorimetry using a Turner Design 10-AU fluorometer following the protocol of Strickland and Parsons (1997). Data recorded at 3m depth were used for analysis.

2.2.2. Long-term in situ experimental design

At sea, 54 mussels collected on site were put in a cage and fixed to the SOLA buoy at 3 m depth in June 2020 (Fig. 1A). This cage was lost during a storm in December 2020. A second cage, containing 75 mussels (44.3 $\pm$ 8.8 mm), was installed from December 2020 to June 2021. In SL and CSN lagoons, respectively 134 mussels (50.1 $\pm$ 6.6 mm) and 68 mussels (45.4 $\pm$ 3.9 mm) were placed in a cylindrical cage from June 2020 to June 2021. At SL lagoon, mussels collected from the seawater inlet of Port Leucate were installed in a weighted cage which was placed ~40 cm below the water surface at Port Fitou, in the same area used in Andrisoa et al. (2019) (Fig. 1B). At CSN lagoon, the weighted cage was filled with mussels collected on site and submerged ~30 cm below the water surface. The cage was located on the eastern side of the lagoon, nearby the Village des Pêcheurs (Fig. 1C).

Once a month, mussels were immersed for 1 h in a calcein solution (150 mg/L), a fluorochrome that is incorporated into the calcium-carbonate structure of the shell (Moran and Marko 2005). To calculate their condition index (CI), eight mussels were sampled each month at SL lagoon and at sea, and six at CSN lagoon, as the number of mussels initially deployed was lower. In CSN lagoon, there was a gap in the calcein staining from October 2020 to January 2021 (i.e. during 4 months) due to turbidity and higher sea level, which prevented the recovery of the cage. In June 2021, all remaining mussels were sampled at each location for sclerochronological analysis (summary of number of mussels used for analysis in Table S1).

Throughout the year, the water temperature was measured every 30 min by a sensor device placed in the cage at each location. Wind speed and orientation data were retrieved from the station "Perpignan", of the French meteorological service (Météo France) with a sampling rate of 3 h. At sea, weekly measurements of salinity, chlorophyll *a* concentration, oxygen and pH were extracted from the SOMLIT database (https://www.somlit.fr/) of the SOLA buoy (Cocquempot et al., 2019). For Mediterranean lagoons, environmental data were provided by the Pôle-relais lagunes méditerranéennes and the FILMED network with a sampling rate of once per month at SL (i.e. salinity, pH and water level) and every two weeks measurements at CSN lagoon (i.e. salinity, pH and oxygen).

2.3. Biomineralisation gene expression

2.3.1. Identification of target genes

Several genes involved at different levels of the biomineralisation process were targeted (Table S.2). Briefly, the genes targeted were *Plasma membrane calcium ATPase* (*Ca-ATPase*), *Carbonic anhydrase*, *Chitin synthase*, *Chitinase*, *Tyrosinase*, *Perwalpin*, *Nacrein* and *Bone morphogenic protein 2* (*BMP2*). Of these, *Ca-ATPase* and *Carbonic anhydrase* are related to the mineral formation. PLASMA MEMBRANE CALCIUM ATPASE is known to transport calcium ions, thereby increasing the concentration of calcium ions in the extrapallial fluid (EPF) (Hüning et al., 2013). CARBONIC ANHYDRASE is an enzyme that forms HCO_3^- from CO_2 and H_2O. The HCO_3^- binds with calcium ions to form the mineral part of the shell, the calcium carbonate. In addition, three genes involved in chitin metabolism were targeted. Chitin is a major polysaccharide that forms the framework for the formation of nacre tablets (Addadi et al., 2006; Engel 2017). CHITIN SYNTHASE is involved in chitin synthesis and CHITINASE in chitin remodelling (Engel 2017). TYROSINASE has a chitin binding domain and is recognised to correct chitin remodelling (Miglioli et al., 2019). Two potential inhibitors of the mineral formation process were also targeted. PERLWAPIN was first observed between the nacre tablets of the abalone *Haliotis laevigata* (Treccani et al., 2006). It consists of a succession of WAP (Whey Acidic Protein) domain sequences that may inhibit the nacre growth. In *M. galloprovincialis*, PERLWAPIN was identified, WAP domains were conserved but their function in calcium carbonate deposition is unknown (Marie et al., 2011). NACREIN was first identified in the nacreous layer of *Pinctada fucata* and later also in the prismatic layer as well (Miyamoto et al., 1996; Miyashita 2002). The protein is composed of two domains, one acting as carbonic anhydrase and the other possibly inhibiting the calcium carbonate precipitation (Miyamoto et al., 2005). The last gene was the one coding for the BMP2, which is known to regulate the biomineralisation, among other functions (Miyashita et al., 2008; Zhao et al., 2016). Housekeeping genes used in this study were *α-Tubulin*, *Actin*, *EF1α, HPRT1* and *RPL7*.

For mRNA sequences not yet identified in *M. galloprovincialis*, a basic alignment search tool (BLASTn on Genbank) was used on sequence read archives (accession number SRX1240182) of the target species using known sequences of closely related species available on Genbank (Table S2). The consensus sequence was constructed using the matching reads and the software BioLign (v 2.0.9.1) (Hall 2001). For cross-validation, blasts (i.e. blastx) were achieved on the later released partially annotated genome of *M. galloprovincialis* (CGA_900618805.1, Gerdol et al., 2020).

2.3.2. In situ hybridization

Mussels were sampled in the bay of Banyuls-sur-Mer at 10 a.m. on April 5, 2021 and sacrificed at noon. The posterior edge of the mantle was sampled and fixed in 4% paraformaldehyde (PFA) in phosphate buffer saline (PBS) at 4 °C. Tissues were dehydrated in a graded ethanol series (70, 95, 100%), dipped in toluene for 3 min and then in

Paraplast® (Merck, Darmstadt, Germany) at 60 °C; after 15 h of impregnation, they were embedded in a new bath of Paraplast®. Eight micrometres thick sections (using a MicroM HM 340^{E} microtome, Thermo Fisher Scientific, Waltham, MA, USA) were laid on glass slides (coated with a 2 % solution of 3−aminopropyl-triethoxy-silane). Prior to *in situ* hybridisation (ISH), sections were successively deparaffinised in toluene, rehydrated (through descending ethanol series) and placed in PBS.

Three genes associated with the biomineralisation process were targeted: *Carbonic anhydrase*, *Chitinase* and *Bmp2* (Table S.3). The sequences were subcloned into a pGEX4T1 expression plasmid (Novagen; EMD Chemicals Inc, PA, USA) containing a GST (glutathione *S*-transferase) tag. Anti-sense (AS) and sense (S) riboprobes were produced using a commercial kit (Roche-Diagnostics DIG labelling kit, Merck, Darmstadt, Germany) according to the recommendations of the manufacturer.

The ISH was performed on proteinase K treated sections using the digoxigenin (DIG) labelled antisense and sense probes, as described elsewhere (Besseau et al., 2006). Briefly, sections were hybridised overnight at 65 °C in a hybridisation buffer containing the probes (1 μg/mL). The sections were then incubated overnight in a solution (1/5000) of anti-DIG antibody conjugated to alkaline phosphatase (Roche, Merck, Darmstadt, Germany). Alkaline phosphatase (AP) activity was detected by the presence of a purple precipitate after incubation with the AP substrate (Roche, Merck, Darmstadt, Germany). Sections were observed using an AxioPlan 2 Imaging microscope equipped with a ProgRes® CF^{cool} camera.

2.3.3. RNA extraction and quantification

TRIzol-chloroform (Invitrogen, Waltham, MA, USA) total RNA extraction was achieved on mantle samples following the instructions of the manufacturer. For this protocol, tissues were ground and homogenised in 500 μL of TRIzol using the FastPrep-24 5G (MP Biomedicals, Irvine, CA, USA). DNase treatment was applied using the DNA-free™ kit (Ambion; Austin, TX, USA), following the protocol of the manufacturer. Concentration and purity were estimated using a NanoDrop spectrophotometer (Nanodrop Technologies, Wilmington, DE, USA) and an Agilent 2100 bioanalyzer (Agilent Technologies, Santa Clara, CA, USA). Gene expression was assessed using the NanoString nCounter™ Gene Expression Assay (NanoString Technologies, Seattle, WA, USA) at the Pôle Technologique CRCT (Toulouse, Fance). The set of probes used was designed by IDT (Integrated DNA Technologies, Coralville, IA, USA) based on sequences retrieved or described in this study (Table S.4). The number of mRNAs counted was normalised following the guidelines of the manufacturer (NanoString Technologies Inc, 2017). The housekeeping gene *HPRT1* could not be used due to low number of transcripts.

2.3.4. Gene expression rhythm

Rhythmicity of genes expression was assessed using the "DiscoRhythm" and "RAIN" packages (Thaben and Westermark 2014; Carlucci et al., 2020) in R (v. 4.1.2) (R Core Team 2020). The package "DiscoRhythm" uses the cosinor adjustment. The acrophase (φ) and the amplitude (A) data were retrieved from this adjustment. The package "RAIN", a non-parametric method, was also used to fit biological data with curves of different shapes. (Thaben and Westermark 2014). The tidal range was defined as 12 ± 2 h and the daily range as 24 ± 4 h (Tran et al., 2020). When gene expression showed both tidal and daily significant rhythms, it was qualified as bimodal. Multiple testing deviations were applied using Benjamini-Hochberg corrected p-value of 0.05 (Benjamini and Hochberg 2000).

2.4. Sclerochronology

2.4.1. Shell preparation

Soft tissues were removed from the shells and the state of the gonads was checked visually (i.e. empty *vs* full). When the gonads were full, the sex was determined by eye. Both tissues were dried separately in an oven at 65 °C for 24 h and weighed. The ratio of tissue dry weight to shell dry weight was calculated in order to obtain the condition index (CI) of the organism (Davenport and Chen 1987; Andrisoa et al., 2019).

Shells were cut from the umbo to the posterior margin on the axis of maximum growth and mounted on a microscope slide (Fig. 2A). Slides of 0.5 mm thickness were cut using a Buehler Isomet low-speed saw (Buehler, Lake Bluff, IL, USA). The cut shells were ground with 120, 240, 600 and 1200 grit silicon carbide paper and polished using Al_2O_3 powder consecutively of 3, 1 and 0.3 μm (Nedoncelle et al., 2013). Calcein marks were visualised using an epifluorescence microscope (Olympus BX61, Olympus Corporation, Tokyo, Japan) by exciting the fluorochrome with blue light at 495 nm (Fig. 2B). The reemission wavelength of calcein is at 515 nm (green).

The increments were revealed using Mutvei's solution, which produces a filigree three-dimensional relief of organic resistant (growth lines) and calcified depressions (growth increments) (Fig. 2C). It consists of 500 mL of 1 % acetic acid, 500 ml of 25 % glutaraldehyde, and 5 g of alcian blue powder. Slides were incubated in the solution for 1 h at temperatures comprised between 37 and 40 °C (Schöne et al., 2005c). Treated shell sections were visualised using a camera (SONY DF W X700, Sony corporation, Tokyo, Japan) mounted on a microscope (Leitz DIAPLAN, Leitz, Germany) and reflected light. The software Visilog 6.2 Noesis was used for image acquisition.

2.4.2. Growth pattern characterisation

Images were assembled and processed using the Gimp and ImageJ software. For each animal collected in June 2021, the distance between the monthly calcein marks along the external side of the shell was measured in order to quantify growth per month. The number of increments between monthly calcein marks was counted twice. The readability of the increments was rated. Each increment of one shell was assigned an arbitrary score between green, orange and red, with green representing clearly readable increments and red representing poorly readable zones (Fig. 2C). Green increments were given a score of two, orange a score of one and red a score of zero. Therefore, the score of the area where all increments are classified as green was 200. Rates were transformed into a coefficient of certainty between 1 and 0 by dividing the score by 200. The coefficient of certainty was calculated for each month and mussel:

(2 x number of green + 1 x number of orange + 0 x number of red)/200 (1)

2.4.3. Statistical analysis

Outliers were searched for and removed for each environmental and biological variable using a Grubbs test (package "outlier" on R (Komsta 2011)). The monthly mean of each environmental and biological variable was computed per location. Variables were compared per studied area using Pearson correlation as implemented in R (v.4.1.2) (R Core Team 2020). The arbitrary confidence level of 0.7 of coefficient of certitude was chosen as a threshold to discard parts of the observed growth patterns not sufficiently readable and to increase the power of the statistical tests.

To define the incrementation regime at the annual and monthly scales, a T-test was applied to the number of increments counted per mussel at each location. The number of observed increments formed by the population, based on confidence level measurements greater than 0.7, was compared with the expected number of increments in the different tidal regimes (Mirzaei and Shau-Hwai 2016). The incrementation regime categories were tidal increments (i.e. one per 12.4 h), daily increments (i.e. one per 24 h), and an intermediate number of increments between 1 and 2 per day, which likely reflects the regional tidal regime (i.e. mixed tidal regime).

Simple linear regressions were made to determine the number of increments formed as a function of the shell growth. Outliers were

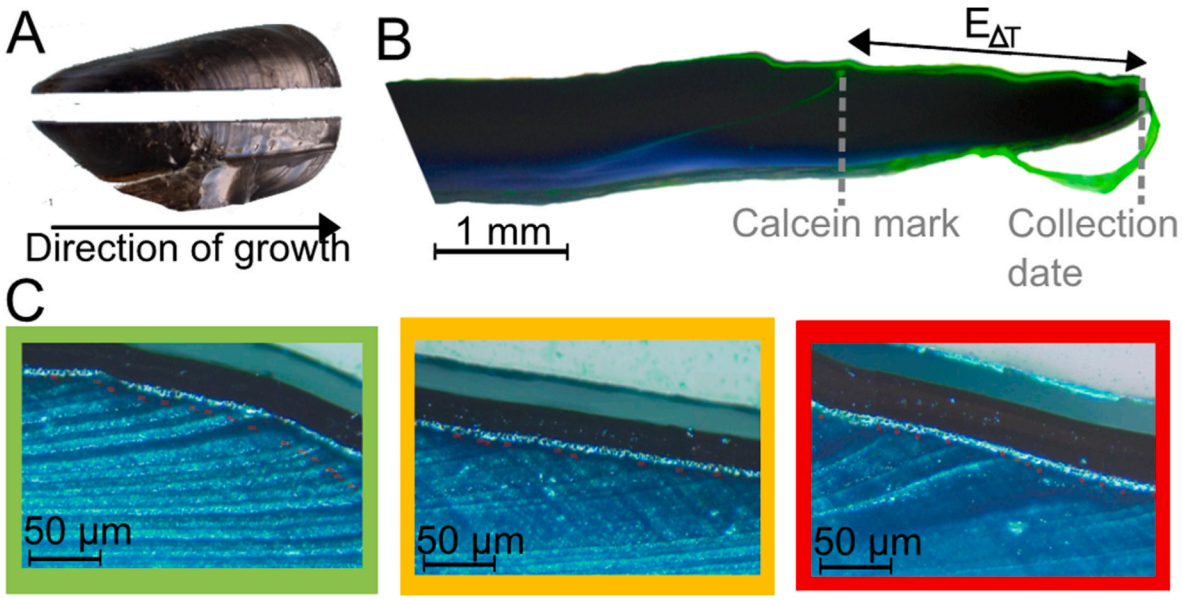

Fig. 2. Shell preparation for growth pattern analysis. (A) Shells were cut from the umbo to the posterior margin along the axis of maximum growth. (B) Calcein mark revealed by fluorescence microscopy. The growth of the shell over a known period of time ($E_{\Delta T}$) was measured between the calcein mark in green and the posterior margin of the shell. The periostracum surrounding the shell showed some autofluorescence. (C) Growth patterns were revealed using a Mutvei treatment. The lecture of the growth patterns was rated in three categories according to their readability. The green category contains clear growth patterns, the orange category contains partially readable growth patterns and the red category contains unreadable growth patterns.

removed using a Grubbs test in R. Normality of the data was assessed using a Shapiro-Wilk test and, if not fulfilled, a logarithmic correction was applied. This was done for all data points at each location but also per regime of incrementation (i.e. tidal, daily and mixed tides).

Normality and homogeneity of the variance of the data were assessed using a Shapiro-Wilk and Leven's tests ("Car" package in R (Fox and Weisberg 2019)). When both conditions ($\alpha \geq 0.05$) were respected, one-way ANOVA was used to assess the difference in CI and growth rate within the same location between months and also between locations at the annual level. If the conditions were not respected, the Kruskal-Wallis rank sum test was used based on the "dunn.test" package in R (Dinno 2017).

3. Results

3.1. Short-term (i.e. daily) experiments

3.1.1. Identification of targeted genes

The targeted sequences were retrieved from NCBI or built using Blast on the *M. galloprovincialis* sequence read archive (Table S2). The sequence encoding *carbonic anhydrase II* was already available on NCBI (KT818923). For the *plasma membrane calcium-transporting ATPase* (*ca2*$^{+}$*ATPase*) mRNA sequence, *M. galloprovincialis* reads were collapsed into a contig of 247 bp based on the gastropod *Haliotis rufescens* sequence (XM_048397027). The translated sequence matched 100% to over 92% of the Ca^{2+} transporting ATPase in the later annotated *M. galloprovincialis* genome (VDI68446). Regarding chitin metabolism, *Chitin synthase* (EF535882) was already described in NCBI for *M. galloprovincialis*. The *Chitinase* contig was constructed from the *M. edulis* sequence (MG827131) and was 201 bp long. The nucleotide sequence was 100 % identical to the *chitinase-like protein*-1 mRNA of *Mytilus chilensis*, validating the contig. The *Tyrosinase* mRNA sequence was assembled using the *tyrosinase-like* sequence of *Mytilus coruscus* (KP57802) and was 877 bp long. Blast on the Genbank nucleotide sequence did not find a similar sequence, although the search on the translated sequence matched at 100% over the first 69 amino-acids of the Tyrosinase-like protein of *M. galloprovincialis* (OPL33388) from base pair number 2 to 208 on the nucleotide sequence. Therefore, the contig was trimmed to a length of 206 bp. The *perlwapin* mRNA sequence was already available on NCBI (FL494664, Venier et al., 2009). A Nacrein-like protein was identified in the shell of *M. galloprovincialis* and the *nacrein* sequence was available in databases (KP670943, Gao et al., 2015). Last, *Bmp2* contig of 176 bp was obtained based on the sequence of the clam *Sinonovacula constricta* (MH822126). The translated amino acid sequence had 100% of identity with the translation of *BMP2/4* annotated gene in *M. galloprovincialis* genome (VDI49543 and VDI49544).

3.1.2. Location of biomineralisation genes expressed in the mantle of *M. galloprovincialis*

Transverse sections of the posterior edge of the mantle, viewed under *in situ* hybridisation, revealed cellular expression of the three tested genes in distinct areas of the mantle sampled at midday (Fig. 3). All target genes were expressed in the basal bulb (BB) and none in the middle lobe (ML). The *Chitinase* gene was expressed in the connective tissue of the inner lobe (IL) and a discrete signal was observed in the inner part of the outer lobe (OL) (Fig. 3B). *Bmp2* transcripts were present at the edge of the basal bulb (BB) and in the connective tissue of the IL (Fig. 3C). *Carbonic anhydrase* (*CA*) expression was also detected in the basal bulb (Fig. 3D) and along the calcifying epithelium (Fig. 3E) and the inner part of the OL. No signal was detected on histological sections treated with sense probes, which served as a negative control (Fig. S.1).

3.1.3. Rhythms of expression of biomineralisation genes in mussels from the bay of Banyuls at short time scale

Large inter-individual variability was observed for all genes studied. Among the targeted biomineralisation genes, most showed similar profiles of expression at the posterior edge of the mantle with tidal or bimodal (i.e. tidal and daily) expression (Fig. 4, Table S.5). *Carbonic anhydrase* (RAIN, $\tau = 12h$, $p = 0.003$), *Bmp2* (RAIN, $\tau = 12h$, $p = 4.9e\text{-}5$), *Chitin synthase* (Cosinor, $\tau = 13h$, $p = 3.2e\text{-}4$), *Chitinase* (Cosinor, $\tau = 14h$, $p = 0.011$), *Perlwapin* (RAIN, $\tau = 12h$, $p = 1.4e\text{-}4$) and *Tyrosinase* (RAIN, $\tau = 12h$, $p = 0.004$) had a main tidal expression with a first peak of expression between 6 p.m. and 8 p.m. and a second between 6 a.m. and 8 a.m. (Cosinor, $p > 0.05$), and then a daily rhythm, except for *Chitinase* which did not show such an imbricated daily oscillation.

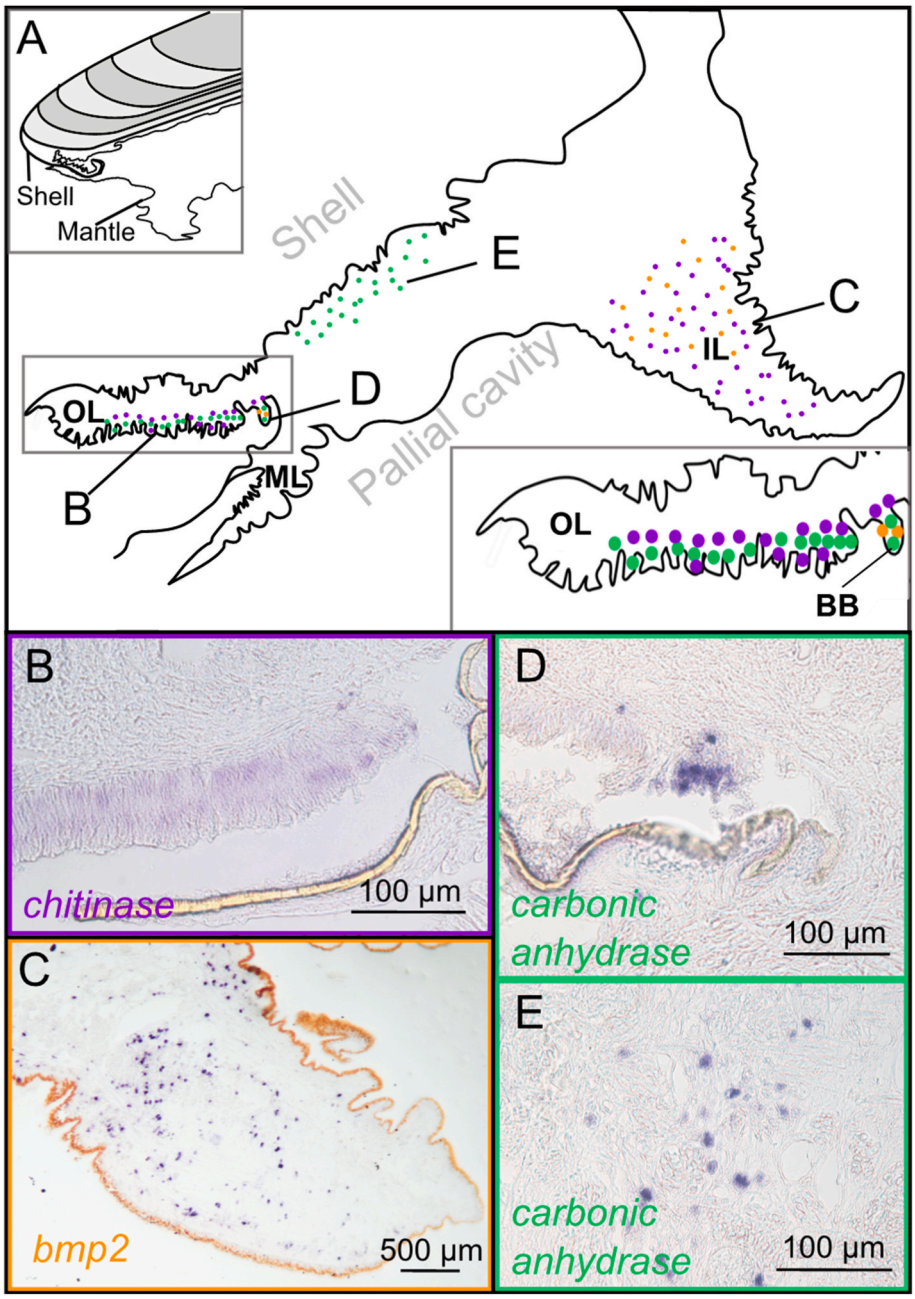

Fig. 3. Expression of *chitinase, bmp2* and *carbonic anhydrase* in the posterior edge of the mantle revealed by *in situ* hybridisation using digoxigenin labelled RNA probes. (A) Summary of observed gene expression in the posterior edge of the mantle. The top left figure shows the portion of the mantle tissue studied. The bottom left figure represents a zoom of the outer lobe (OL) (B) Expression of *Chitinase* in the OL as revealed by alkaline phosphatase activity, which forms a purple precipitate. (C) Expression of *Bmp2* in the inner lobe (IL). (D) Zoom on the expression of *Carbonic anhydrase* in the basal bulb (BB) and (E) along the calcifying epithelium. No biomineralisation gene expression was observed in the middle lobe (ML).

Nacrein showed both tidal (Cosinor, $\tau = 12h$, $p = 3.7e\text{-}4$) and daily oscillations (RAIN, $\tau = 20h$, $p = 0.008$) with an acrophase at 12:25 p.m. (Cosinor, $p = 3.7e\text{-}4$) and 6:40 a.m. respectively. (Cosinor, $p > 0.05$). The last biomineralisation related gene studied, *Ca^{2+}ATPase* had only a daily oscillation (RAIN, $\tau = 20h$, $p = 5.2e\text{-}5$) with an acrophase at 11:45 p.m. (Cosinor, $p = 0.003$).

3.1.4. Environmental dynamic in the bay of Banyuls at short time scale

During the 36-h experiment in the bay of Banyuls, the sun rose at 7:20 a.m. and set at 8:10 p.m., with a peak in solar intensity at 1:44 p.m. (Fig. S.2). High tides occurred at 1:55 p.m., 1:14 a.m. and 3:19 p.m., a classic profile for a mixed tidal regime. Physico-chemical measurements showed that the chlorophyll *a* and pheophytin concentrations oscillated in antiphase with the tides, although the variations in concentrations were small (i.e. Δ [Chl *a*] = 0.11 mg/m^3 and Δ[pheo] = 0.013 mg/m^3) (Fig. S2). Temperatures decreased slightly over the 36 h, dropping from 20.11 °C at 12:00 p.m. to 19.85 °C at 8:00 a.m. Salinity also decreased by 0.11 ‰ during the sampling period.

3.1.5. Comparison of gene expression rhythms with environmental dynamics on a short time scale

Chitinase, *Tyrosinase*, *Carbonic anhydrase*, *Chitin synthase* and *Perlwapin* had a peak of expression around low tides and therefore around higher concentrations of chlorophyll *a* and pheophytin. The rhythm of *Nacrein* expression was not in phase with the group of genes and showed higher expression around high tides. Temperature and salinity

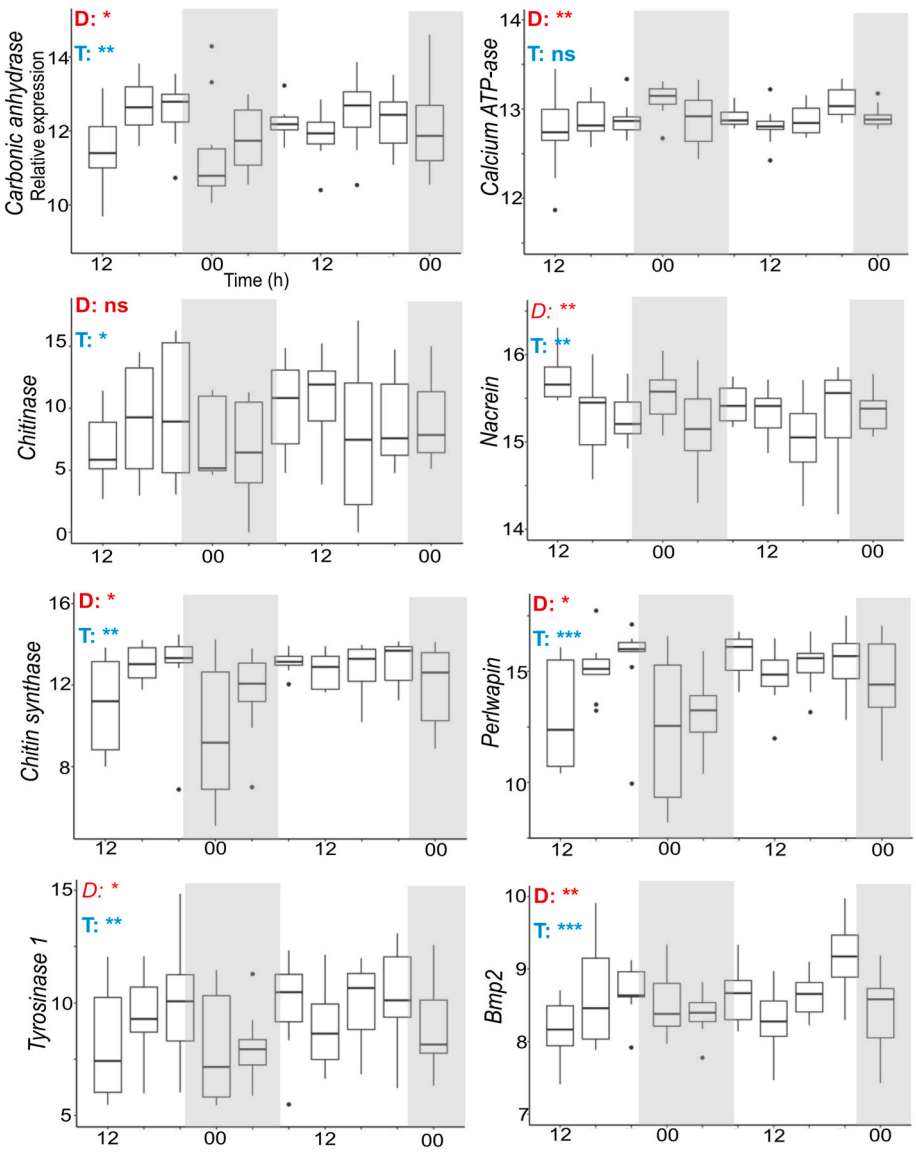

Fig. 4. Variation of biomineralisation gene expression over time in mussels from the bay of Banyuls. Grey shading indicates the dark phase and white the light phase. Daily (D, 24h ± 4, in red) and Tidal (T, 12h ± 2, in blue) rhythms of gene expression were tested. Cosinor adjustment and RAIN analysis were achieved to test the rhythmicity of gene expression. When two adjustments were significant, the significance level is shown in bold. When only one was significant, the significance level is shown in italics. Significance levels: ns: $p > 0.05$; *: $0.05 \geq p \geq 0.01$; **: $0.01 > p \geq 0.001$; ***: $p < 0.001$.

variations did not induce variations in the expression of biomineralisation genes.

3.1.6. *Shell growth patterns of M. galloprovincialis in September 2020*

The mussels analysed were part of the first cage deployed at sea, which was lost in December 2020. For the five mussels collected in September 2020, shell growth patterns were readable for three individuals over the target period (confidence level >0.7). On average, 89 ± 6 increments were formed over 47 days, corresponding to an average of 1.9 ± 0.1 increments.d^{-1} (Fig. 5A–C). From the August 24, 2020 (last calcein labelling of the mussels) to October 9, 2020 (mussel collection), 81 cycles of high and low tide occurred in the bay of Banyuls-sur-Mer instead of 91 in the semidiurnal tidal regime (Fig. 5D). The *t*-test confirmed that incrementation regime was tidal during this period.

3.2. *Long-term (i.e. yearly) experiment*

3.2.1. *Condition index of M. galloprovincialis*

The ratio between soft and hard tissue was used to calculate the condition index (CI) of the mussels. Over the year at sea, the CI was significantly lower in January and February (mean CI = 12 ± 2; χ^2, n = 65, $p < 0.05$) than in May and June (mean CI = 18 ± 3) (Fig. 6A). Interestingly, the CI increased significantly in March (mean CI = 17 ± 3), which was similar to the values of the summer months, before decreasing in April (mean CI = 10 ± 1). The condition index of mussels from SL lagoon described a significant seasonal trend with higher values in December–January (mean CI = 13 ± 2; χ^2, n = 130, $p < 0.05$) and lower values in May–June (mean CI = 6 ± 1) (Fig. 6B). Although data were missing in autumn (see Methods), a seasonal trend was suggested for mussels from CSN lagoon (χ^2, n = 67, $p < 0.05$), with higher values in summer (i.e. July to September, mean CI = 24.3 ± 4.3) and lower values in winter (i.e. January to March, mean CI = 10 ± 2) (Fig. 6C). In all environments, a decrease in CI was observed after the presumed spawning event.

Due to the lack of data for the site at sea between June 2020 and December 2020 (see Methods), only the mean CI from January 2021 to June 2021 could be compared between sites. The CI was similar for mussels from the CSN lagoon (mean CI = 16 ± 5) and from the sea

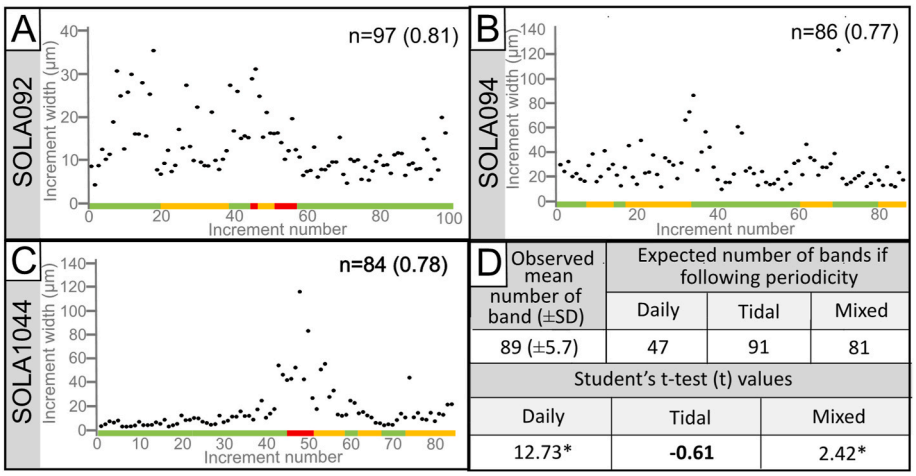

D

Observed mean number of band (±SD)	Expected number of bands if following periodicity		
	Daily	Tidal	Mixed
89 (±5.7)	47	91	81

Student's t-test (t) values		
Daily	Tidal	Mixed
12.73*	**-0.61**	2.42*

Fig. 5. Characterisation of shell growth patterns of *Mytilus galloprovincialis* individuals reared in the bay of Banyuls between August and September 2020. (A–C) Variation of increment width in the shell of 3 mussels. Green, yellow and red bands indicate the readability of the increment (See Fig. 2C). The observed number of increments is given and in parentheses the coefficient of certitude calculated from the increment readability. (D) Comparison of the observed number of increments formed in the shells with the expected value according to the three incrementation regimes. The Student's t-test value in bold is the most probable incrementation pattern formed. When the null hypothesis (HO) is rejected, symbolised by an asterisk (*), the observed number of increments in the population was significantly different from the expected number ($p < 0.05$). Daily: 1 increment per 24 h; Tidal: 1 increment per 12.4 h; Mixed: following the mixed semidiurnal tidal regime of the region.

(mean CI = 14 ± 3) (ANOVA, n = 182, $p > 0.05$), with a higher variability in the lagoon than in the sea. The CI of the SL lagoon mussels was significantly lower and less variable than in the other two locations (mean CI = 9 ± 2) (ANOVA, $p < 0.05$). No significant differences were observed between males and females in the three locations studied (ANOVA, n = 61 (SL), n = 45 (CSN), n = 60 (sea), $p > 0.05$). A significant difference between mussels with full or empty gonads was observed in SL lagoon (χ^2, n = 130, $p < 0.001$), but not in the other two study sites (ANOVA, n = 67 (CSN), n = 65 (sea), $p > 0.05$).

3.2.2. Shell growth rate

Shell growth rates were averaged per month, based on the monthly staining. For each site, there were no significant differences in shell growth rates between months (χ^2, n = 94 (SL), n = 67 (CSN), n = 65 (sea), $p > 0.05$) (Fig. 6). As some periods were missing (i.e. lack of staining in autumn at CSN lagoon, loss of the first mussel cage in December 2020 at sea), the comparison of growth rates between sites was made from January to June 2021 for standardisation. During this period, the mean growth rate was similar in both lagoons (32.5 ± 10.3 µm d^{-1} for SL and 32.1 ± 7.5 µm d^{-1} for CSN lagoon) (ANOVA, n = 31, $p > 0.05$) and significantly higher at sea (mean growth rate: 59.6 ± 10.7 µm d^{-1}) (ANOVA, n = 31, $p < 0.001$). No significant difference was observed between male and female shell growth rates (χ^2, n = 14, $p > 0.05$). An effect of energy allocation to reproduction instead of growth was not observed in either lagoon. However, in the sea, shell growth seems to be lower before spawning, although no significant difference was observed.

3.2.3. Growth increment

The readability of the increments was assessed by classification into three categories to obtain a confidence level per month for each mussel shell (see Methods). The overall mean confidence level was 0.7 ± 0.1 for mussel shells in each site. Mean confidence levels were similar between the studied locations and months (χ^2, n = 153, $p > 0.05$). Shells with too many missing increments and too uncertain retro-dating were removed. Finally, the number of increments formed per day was estimated for each shell individually (Examples Fig. 7) and synthesised on Fig. 6 for the 11 shells at sea, 8 shells at SL lagoon and 8 shells at CSN lagoon that showed adequate increment revelation.

The number of increments formed per day varied depending on the period of the year (Table 1, Table S.6). For the mussels raised at sea, an average of 1.7 ± 0.5 shell increment.d^{-1} was observed in winter. This value decreased to 1.4 ± 0.1 increment.d^{-1} when measurements with a confidence level below 0.7 were excluded. From April to June 2021, the number of increments formed per day was close to or well above 2 increments.d^{-1}. Two groups of growth patterns appeared in the mussels from SL lagoon. The first group consisted of shell increments formed during the summer months with a mean number close to one (e.g. 1.2 ± 0.4 and 1.3 ± 0.4 increment.d^{-1} in summer 2020 and 2021, respectively). The second group consisted of the part of shells formed in winter and early spring, with an average of 1.6 ± 0.5 to 1.7 ± 0.6 increment.d^{-1} from December 2020 to March 2021. In shells from CSN lagoon, the pattern was opposite that in SL, with almost two increments formed per day in spring and summer (mean of 1.9 ± 0.1 increment.d^{-1}), except in June 2021 (average of 1.5 ± 0.4 increment.d^{-1}), and lower in winter (average of 1.2 ± 0.4 increment.d^{-1}). As observed at sea the number of increment formed exceeded 2 increments.d^{-1} in CSN lagoon in July 2020.

The observed number of increments was compared to the expected number of increments if the increment formation was either daily, tidal or following a mixed tidal regime. T-tests showed that in the shells of mussels living at sea, growth increments were formed according to a rhythm close to the mixed tidal regime of the region from December 2020 to March 2021 (i.e. 1.7 ± 0.1 cycle.d^{-1}), and then switched to a tidal rhythm from April to June 2021, with occasional parts of supernumerary increments (e.g. ≥2.5 increment.d^{-1} in April 2021, Table 2). In SL lagoon, one increment per day was formed from July 2020 to October 2020, in April 2021 and in June 2021 (T-test, $p < 0.05$). Between November 2020 and March 2021, the number of increments formed per day is close to the rhythm of the mixed tidal regime. As previously observed, in CSN lagoon the pattern was opposite to SL, with daily incrementation from October 2020 to January 2021. For the rest of the year, the number of increments formed per day appeared to be related to a mixed tidal regime, except in July 2020, when the tidal cycle predominated (Table 2).

The number of increments formed was compared with shell growth using a simple linear regression (Fig. S.3). When all measurements are grouped per site, a weak relationship is observed (at sea, n = 32, R^2 = 0.36, $p < 0.001$; at SL, n = 38, $R^2 = 0.51$, $p < 0.001$; at CSN, n = 29, R^2 = 0.47, $p < 0.001$). The relationship between shell growth rate and

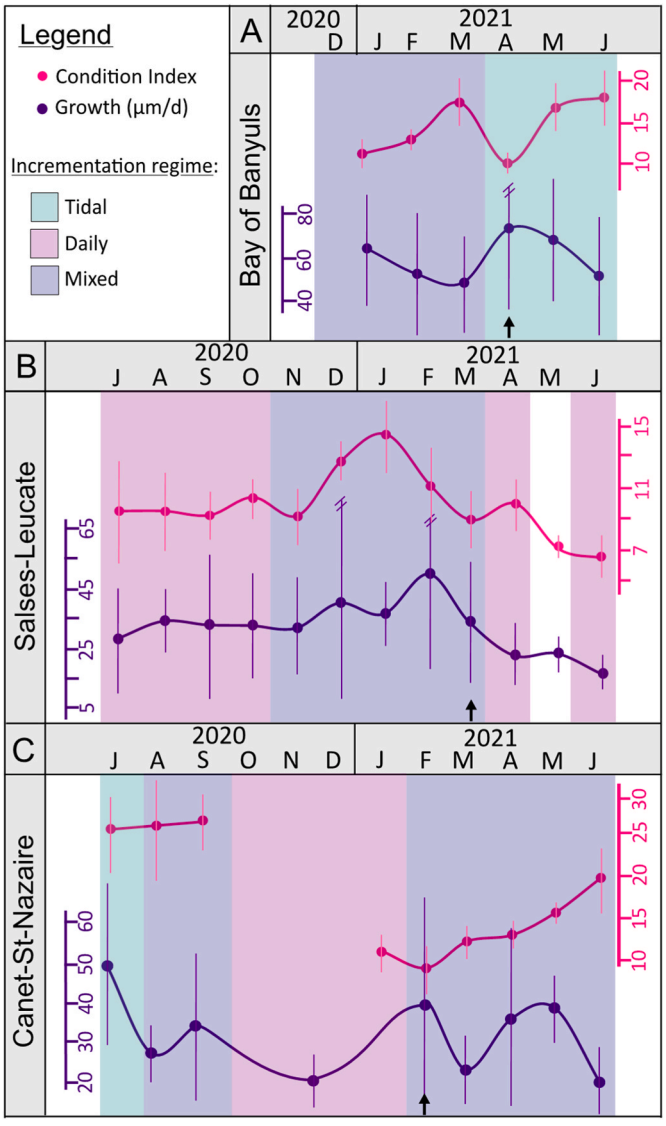

Fig. 6. Monthly average of *Mytilus galloprovincialis* Condition Index (CI) and shell growth rates measured for the three experimental locations. (A) At sea (bay of Banyuls-sur-Mer) and in the Mediterranean lagoons of (B) Salses-Leucate and (C) Canet-St-Nazaire. The pattern of increment formation is deduced from the sclerochronological analysis of the shells. Incrementation regimes were tidal (i.e. 1 increment represents 12.4 h, in light green), daily (i.e. 1 increment represents 24 h, in light pink) and mixed (i.e. semidiurnal tides with diurnal inequality, in light purple). White areas had no significant incrementation regime. Black arrows indicate probable spawning events based on visual observation of the gonads.

number of increments was then characterised for each site during periods associated with the different growth patterns observed (i.e. daily, tidal and mixed tidal regime). At SL lagoon, the growth rate explained 84% of the variation observed in the number of increments during periods associated to a mixed tidal regime ($n = 16$, $R^2 = 0.84$, $p < 0.001$), but no relationship was observed during the period of daily incrementation ($n = 14$, $R^2 = 0.02$, $p > 0.05$). A small relationship was observed for shells from CSN lagoon during the period of mixed tidal increment formation ($n = 24$, $R^2 = 0.38$, $p < 0.001$), whereas at sea the number of shell increments can be weakly but significantly related to shell growth rate when growth pattern is tidal ($n = 18$, $R^2 = 0.39$, $p < 0.001$).

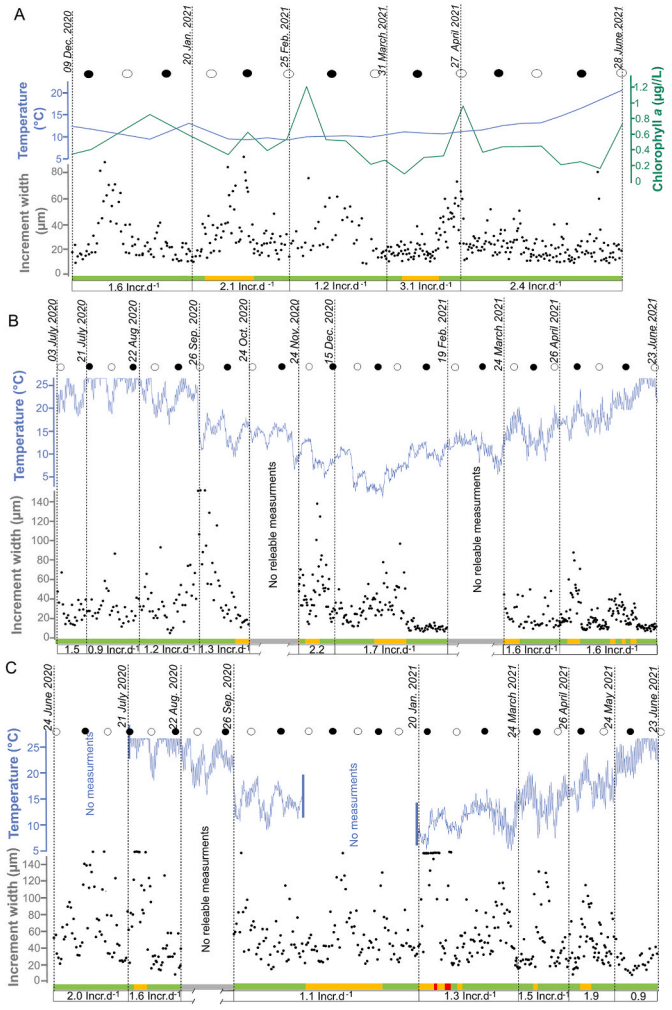

Fig. 7. *Mytilus galloprovincialis* shell growth in relation to the environmental variations in the three Mediterranean environments studied. (A) The bay of Banyuls with specimen SOLA0624, (B) the Salses-Leucate lagoon with specimen SL0601 and (C) Canet-Saint-Nazaire lagoon with specimen CSN0602. The dates of the visible calcein marks are used to delimit the number of increments formed per day within the interval. Green and yellow bands indicate the confidence level of the increment lecture. The blue profile corresponds to the recorded temperatures and the green profile the chlorophyll *a*. The lunar cycle is represented by black and white circles (i.e. empty and full moon).

Table 1
Mean number of increments formed per day in shells of mussels reared in the three studied environments. Measurements below 0.7 of confidence level were removed.

	SOLA (at sea)	SL	CSN
07/20		1.3 ± 0.4	2.3 ± 0.3
08/20		1.2 ± 0.4	1.8 ± 0.4
09/20	ND	1.3 ± 0.4	1.5 ± 0.3
10/20		1.5 ± 0.4	
11/20		1.4 ± 0.4	1.2 ± 0.4
12/20		1.6 ± 0.5	
01/21	1.4 ± 0.1	1.7 ± 0.2	
02/21	1.5 ± 0.3	1.6 ± 0.5	1.4 ± 0.4
03/21	1.7 ± 0.5	1.7 ± 0.6	1.5 ± 0.6
04/21	2.5 ± 1.0	1.3 ± 0.4	1.7 ± 0.4
05/21	2.1 ± 0.4	1.4 ± 0.1	1.9 ± 0.4
06/21	2.1 ± 0.5	1.3 ± 0.3	1.5 ± 0.4

Table 2
Differences between expected and observed number of increments formed monthly at sea and in Salses-Leucate and Canet-Saint-Nazaire lagoons. Only measurements of shell increments having a confidence level >0.7 were used in this test. Student's t-test (t) values are given. In bold numbers were the most probable incrementation pattern formed, closer the value was to zero, more the mean observed number of increments was close to the expected value. When the null hypothesis (HO) rejected, symbolise by an asterisk (*), the observed number of increments in the population was significantly different than the expected number ($p < 0.05$). Daily: 1 increment per 24 h; Tidal: 1 increment per 12.4 h; Mixed: following the mixed semidiurnal tidal regime of the region.

	SOLA (at sea)			Salses-Leucate lagoon			Canet-Saint Nazaire lagoon		
	Daily	Tidal	Mixed	Daily	Tidal	Mixed	Daily	Tidal	Mixed
07/20				**1.83**	−4.78*	−3.61*	9.08*	**2.47**	3.00
08/20				**1.20**	−5.21*	−4.81*	4.47*	−0.89	**−0.54**
09/20	ND			**1.66**	−5.86*	−4.26*	5.01*	−3.60*	**−2.30**
10/20				**2.12**	−5.41*	−3.96*			
11/20				2.47	−2.65	**−1.06**	**1.48**	−5.03*	−3.29*
12/20	5.39*	−3.42*	**−0.26**	3.01	−1.62	**−0.23**			
01/21				7.23*	−2.76	**1.35**			
02/21	4.07*	−3.48*	**−1.48**	2.94	−1.63	**−0.98**	2.51	−3.01	**−2.22**
03/21	4.32*	−1.24	**−1.06**	2.81	−1.20	**−0.40**	2.46	−1.85	**−0.98**
04/21	3.93*	**1.24**	1.67	**1.55**	−4.17*	−4.62*	3.76*	−1.20	**−0.72**
05/21	7.72*	**1.73**	2.42	7.55*	−9.16*	**−7.23***	4.54*	−0.33	**0.23**
06/21	4.07*	**0.55**	0.88	**2.36**	−6.11*	−5.21*	2.78	−2.99	**−2.37**

3.2.4. Environmental dynamics at each study site

The values of the measured environmental variables were averaged on a monthly scale in order compare and describe them for the three experimental locations (Tables S6, S7 and S8). In all environments, temperatures showed a seasonal variation. At sea, the monthly mean temperature varied between a maximum of 22.2 °C in summer and a minimum of 11.8 °C in winter. In both Mediterranean lagoons, mean temperatures varied from 23.7 to 25.9 °C in summer to 5.6 and 6.5 °C in winter for SL and CSN, respectively. No seasonality was observed for salinity, but the values were lower and more variable in the lagoons (mean salinity at SL = 33.7 ± 1.9 ‰ and at CSN = 32.4 ± 3.5 ‰) than in the sea (mean salinity = 37.6 ± 0.4 ‰). The pH was relatively stable throughout the year at sea and in CSN lagoon (mean pH = 8.0 ± 0.1 and 8.2 ± 0.1 respectively), whereas it was more variable and higher in SL lagoon (mean pH = 8.3 ± 0.2). At sea and in SL lagoon, the chlorophyll *a* concentration was variable but without a clear cyclic profile (mean Chl *a* = 0.7 ± 0.4 µg.L^{-1} at sea and 0.8 ± 0.3 µg.L^{-1} at SL). At sea, the chlorophyll *a* levels were lower in summer (mean Chl *a* = 0.17 ± 0.1 µg.L^{-1} in July–August 2020) and reached a maximum in November (Chl *a* = 1.63 µg.L^{-1}). In SL lagoon, the chlorophyll *a* level was lowest in September (mean Chl *a* = 0.53 µg.L^{-1}) and in spring (Chl *a* = 0.5 µg.L^{-1} in March and April), while the highest values occurred in January 2021 (Chl *a* = 1.3 µg.L^{-1}). The oxygen level at sea was stable (annual mean O_2 concentration = 5.6 ± 0.4 ml.L^{-1}). In the CSN lagoon, the oxygen concentration showed higher values than at sea and a seasonal range characterised by a winter peak of 11.6 ml.L^{-1} (in January) and a summer decrease of 7.7 ml.L^{-1} (in June).

3.2.5. Shell growth patterns in relation to environmental parameters

The monthly means of the increment rhythms, shell growth rates and condition indices were compared with the environmental parameters (Tables S9, S.10 and S.11).

At sea, chlorophyll *a* and oxygen concentrations were correlated (Pearson correlation = 88, n = 12, $p < 0.05$). Both were negatively correlated with temperature (Pearson correlation = −85 and −92 respectively, n = 12, $p < 0.05$). Shell growth rate was correlated with salinity (Pearson correlation = 84, n = 6, $p < 0.05$). No significant relationship was observed between the type of incrementation regime and the measured environmental parameters (Table S.10).

In the SL lagoon, the pH was positively correlated with temperature (Pearson correlation = 70, n = 12, $p < 0.05$), whereas chlorophyll *a* and condition index were inversely correlated with temperature (Pearson correlation = −65 and 74 respectively, n = 12, $p < 0.05$). Shell growth rate was significantly related to the condition index (Pearson correlation = 68, n = 12, $p < 0.05$; Table S.11). However, no significant relationship was observed between the type of incrementation regime and the environmental parameters. However, the mixed tidal increments were formed when the CI reached its maxima (Fig. 6).

In CSN lagoon, O_2 and condition index were inversely correlated with temperature (respectively Pearson correlation = −95 and −97, n = 12 and 9, p = 0.01 and 0.001), while O_2 was positively correlated with pH (Pearson correlation = 45, n = 12, p = 0.05). No significant relationship was observed between shell growth rate and incrementation regime with environmental parameters.

4. Discussion

This study investigated the rhythmicity of shell growth increment formation in *Mytilus galloprovincialis* and its potential drivers using molecular and sclerochronological approaches. First, based on the expression of biomineralisation genes in the mantle, we showed that the process of biomineralisation is rhythmic and probably synchronised to tides. On a large time scale (i.e. annual), we observed that incrementation regime differed between environments and also over the year. However, the incrementation regime observed cannot be fully explained by the environmental variation and we therefore hypothesise that biological clocks may also drive biomineralisation.

4.1. Molecular to sclerochronological evidence of rhythmic shell biomineralisation in Mytilus galloprovincialis

Based on short-term experiment, the expression of genes related to biomineralisation was localised and quantified in the mantle of *M. galloprovincialis* to assess whether the formation of growth increments can be considered as a periodic process. *In situ* hybridisation revealed that the genes B*mp2*, *Carbonic anhydrase* and *Chitinase*, which are thought to be involved in the biomineralisation process, were expressed in tissues of the posterior edge of the mantle connected to the ventral margin of the extrapallial cavity.

Gene expression levels showed high inter-individual variability, which was expected when studying shell growth in *M. galloprovincialis* (Fuentes-Santos et al., 2018; Prieto et al., 2019). Furthermore, previous studies on rhythmic valve activity in *M. galloprovincialis* showed that individuals from the same population were poorly synchronised (Comeau et al., 2018; Bertolini et al., 2021). Despite a high inter-individual variability, in mussels collected at sea, the expression of most genes followed a tidal variation with a peak associated to low tides, excepted for *Nacrein,* which showed a peak of expression during high tides. Tidal expression of genes involved in biomineralisation has previously been reported for bivalves, such as *Carbonic anhydrase* in the mussel *Mytilus californianus* (Connor and Gracey 2011) and *Nacrein* in the pearl oyster *Pinctada fucata* (Miyazaki et al., 2008). Our

sclerochronological analysis revealed tidal incrementation in the shell of mussels, suggesting that the genes we targeted may be directly involved in the rhythmic formation of shell growth increments. Therefore, the biomineralisation process in *M. galloprovincialis* can be considered as rhythmic and we can assume that the time needed to form of one increment and one growth line is stable and equal to 12.4 h.

4.2. Different growth patterns are observed in the shells of *M. galloprovincialis*

While the expression of biomineralisation genes and the deposition of shell increment in *M. galloprovincialis* from the Mediterranean Sea appear to be linked on a short time scale (i.e. days), the growth pattern changes with time, including within the same individual, over longer-term observations (i.e. a year). Analysis of shell growth patterns on an annual scale revealed that the unit of time imbedded in shell increment varied according to the period of the year and to the type of environment. At sea, increment formation shifted from tidal to mixed tidal regime, a pattern likely related to the type of tidal regime that characterises this area of the Mediterranean Sea. In both Mediterranean lagoons, the shell incrementation regime was different from that of mussels at sea, with a shift between daily and mixed depending on the period of the year. Surprisingly, the shells of *M. galloprovincialis* did not show any seasonal variation or annual cessation of growth, which is unusual for bivalves (Louis et al., 2022).

The previous studies on bivalve shells from the Mediterranean Sea, both conducted in marine lagoons of the French coast (i.e. at Thau and Salses-Leucate lagoons), described daily growth patterns for the oyster *Magallana gigas* (Langlet et al., 2006) and the mussel *M. galloprovincialis* (Andrisoa et al., 2019). These observations are consistent with the daily growth increments occasionally observed in the present study in the Salses-Leucate and Canet-Saint Nazaire lagoons. However, increments following tidal and regional mixed tidal regimes have never been observed in organisms inhabiting the Mediterranean Sea. Unconventional incrementation regimes in bivalve shells have been already reported (see Louis et al., 2022 for review), but are more likely to reflect aperiodic increments, likely related to weather-scale phenomena such as storms and cyclones (Yan et al., 2020; de Winter et al., 2023).

The readability of increments in subtidal mussel shells is classically low compared to intertidal bivalve shells, resulting in differences between the expected and observed number of increments (Richardson et al., 1989; 1990). In our study, the mixed regime recorded in the growth pattern is observed in shells with clear readability of growth increments. It is therefore unlikely that the mixed pattern results to growth lines counting bias.

4.3. Environment alone cannot explain observed differences in shell growth patterns in *M. galloprovincialis*

At the locations studied, the tides are associated with a weak tidal range ($\leq$30 cm in the bay of Banyuls and $\leq$10 cm in the lagoons), and with a mixed tidal regime (SHOM, 2020). The small-scale molecular study showed that the expression of biomineralisation genes was related to the tides. Therefore, the mixed growth increments formed are likely to be related to the tidal regime of the region. To our knowledge, a link between shell increments and mixed tidal regime has only been suggested by Nedoncelle et al. (2013) for the deep-sea mussel *Bathymodiolus thermophilus* from the East Pacific Rise. Based on an *in situ* mark-recapture experiment, the authors described that the circalunidian rhythm (i.e. ~24.8 h) is the basis for shell increment formation, but changes in increment deposition with time occurred through the formation of a faint line, leading to periods with 2 increments per day and periods with only one increment per day. This is likely to correspond to mixed semidiurnal tidal increments, consistent with the mixed semidiurnal tidal regime of this area in the Pacific (SHOM, 2020). Tides generate local environmental changes such as current speed and direction, water temperature, light intensity or food fluxes (Saurel et al., 2007; Roberts et al., 2018). However, the environmental data measured in our study do not allow us to determine which component is predominant for driving shell increment formation.

Tidal increments (i.e. one increment and one growth line formed every 12.4 h) have previously been described in *Mytilus* shells, including *M. edulis* (Richardson 1989; Buschbaum and Saier 2001) and *M. galloprovincialis* (Tanaka et al., 2019). However, mussels with tidal incrementation classically originate from tidal habitats with a semidiurnal regime (i.e. regular cycles of 12.4 h) (Richardson 1989; Buschbaum and Saier 2001; Tanaka et al., 2019), which is not the case in the environments studied here. Therefore, the observed tidal incrementation may be independent of local environmental conditions. Based on aquaria and *in situ* experiments, Richardson et al. (1980) and Richardson (1987, 1988, 1989) identified a cyclic deposition of microgrowth bands in the shell of *Cerastoderma edule*, *Ruditapes philippinarum* and *M. edulis*, that was independent of the surrounding tidal regime, suggesting the role of an innate response. This driver, now widely described in the literature, refers to biological clocks and suggests their role in controlling the rhythm of shell increment formation (Schöne 2008; Warter et al., 2018; Sano et al., 2021; Louis et al., 2022). Biological clocks are molecular feedback loops that are set and reset by environmental factors (i.e. zeitgebers such as photoperiod, temperature and food availability) and orchestrate many physiological and behavioural activities (Aschoff 1981; Dunlap 1999). In a constant environment, the system is free-running meaning that physiological and behavioural outputs maintain their cyclical nature. In bivalves, it has been shown that biological clocks can run in a tidal and/or daily mode depending on the environment (Mat et al., 2012; Tran et al., 2020). *Mytilus galloprovincialis* organisms inhabiting non-tidal habitats have been shown to adopt a daily activity, whereas in tidal ecosystems they show a tidal behaviour (Comeau et al., 2018; Trusevich et al., 2021). Therefore, daily and tidal increments observed in Mediterranean lagoons and at sea, respectively, could be driven by biological clocks.

4.4. Proposition of a hypothetical model of the increment formation in *Mytilus* shells

Based on the results of this study and previous observations in the literature, we propose a revised model for shell increment formation in *Mytilus* species (Fig. 8). This model is based on the joint effect of the environmental dynamics (in particular the feeding conditions), likely driven by the local tidal system, together with biological clocks.

The current model is based on the sclerochronological analysis of shells from intertidal habitats (Fig. 8A). Mussels are subjected to an alternation of emergence and submergence periods, which are likely to control the formation of well-defined growth bands, as shown by Richardson (1989), Buschbaum and Saier (2001) and Tanaka et al. (2019). It is assumed that growth slowdowns or breaks result from periodic valve closures during emergence phases (Lutz and Rhoads, 1977). At the same time, biological clock(s) have been shown to generate rhythmic outputs, such as valve activity, that follow tidal dynamics (Comeau et al., 2018; Tran et al., 2020). As the biological clocks of bivalves in intertidal systems are strongly related to the tides (Mat et al., 2014), it is unclear whether the resulting increment deposition is directly controlled by the tides or indirectly driven by the clocks reset by the tides. As emersion implies valve closure, masking the true state of the molecular biological clock (Mrosovsky 1999; Helm et al., 2017), the resulting shell growth pattern exhibits a tidal mode related to the semidiurnal tidal regime.

In subtidal habitats, the less contrasting environmental dynamics produce less visible growth bands (Richardson, 1989; this study). Previous studies in tidal areas with a wide tidal range (e.g. Menai Strait, North Wales, UK) have shown that shell increment formation appears to be primarily controlled by the rhythm given by biological clocks, likely leading to semidiurnal increments in semidiurnal tidal ecosystems.

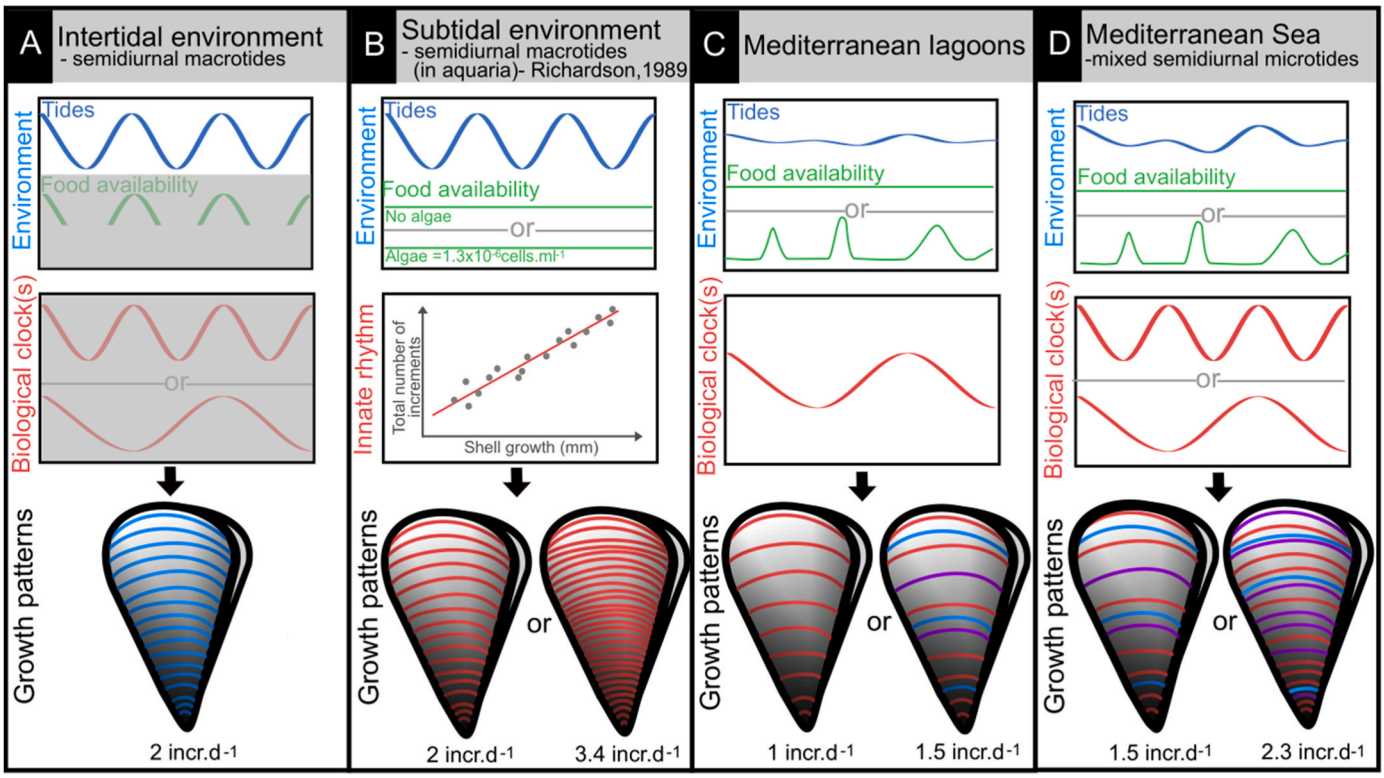

Fig. 8. Hypothetical model of shell increment formation in mussel shells as a function of the environment. The environmental drivers illustrated are tides (blue) and food availability (green). Shell growth increments are also controlled by putative biological clock(s) (red), by the environment (light blue), or both (purple). (A) In intertidal habitats, a growth break occurs when mussels are out of the water. Both the alternation of emersion and immersion periods and biological clocks may act in phase, leading to a tidal rhythm of biomineralisation process. (B) In subtidal habitats subject to a high tidal range, the formation of shell growth increments is primarily controlled by biological clocks running at tidal rhythm. But supernumerary increments occur during periods of high growth rates (based on the model proposed by Richardson (1989)). (C) In Mediterranean lagoons, increments are deposited with a mixed tidal pattern under favourable food conditions, whereas otherwise the biological clock running on a daily scale predominates. Supernumerary growth bands may be related to inconsistencies between biological clocks and environmental cues. (D) In subtidal Mediterranean marine waters, where mussels are exposed to a mixed tidal regime with low range, shell increment deposition alternatively follows a biological clock running at tidal frequency and the local tidal regime when food conditions are not limiting. Asynchronisation of endogenous and environmental cues can results in periods of supernumerary growth bands.

However, changes in environmental conditions can increase or reduce growth, resulting in more or less increments than expected (Richardson et al., 1988; 1989) (Fig. 8B). In his study, Richardson (1989) attributed increment formation to an innate rhythm of band deposition that may be related to structural constraints (i.e. the balance between the amount and disposition of organic and mineral components of the shell, leading to a hard structure that does not break easily). In the 3 locations studied in this paper, no strong relationship was observed between the monthly averaged shell growth rates and the number of increments. Only in some cases, growth rate explained most of the variation observed in the number of increments, as in the case of shells from SL lagoon, during the period of mixed tidal increment formation (i.e. $R^2 > 0.8$). These results indicate that the growth rate alone cannot explain the number of increments formed in the shell of *M. galloprovincialis*.

A double control in the increment formation of *M. galloprovincialis* from the Mediterranean Sea may occur, although it is still unclear why shells from Mediterranean lagoons show an alternation of daily (i.e. endogenous) and mixed semidiurnal (i.e. tide-controlled) growth bands, whereas shells from the sea, located in the close vicinity of lagoons, show an alternation of tidal (i.e. endogenous) and mixed semidiurnal (i.e. tide-controlled) growth bands. The identification of a parameter that induces changes in the shell incrementation regime of *M. galloprovincialis* is not obvious. Interestingly, the two Mediterranean lagoons studied showed opposite shell growth patterns throughout the year (e.g. mixed tidal increments were formed in the shells from SL in winter, whereas shells from CSN formed daily increments during this period), while observing similar environmental variations for most of the variables. Food availability and temperature are recognised as the main environmental factors influencing shell growth in bivalves (Ceccherelli and Rossi 1984; Purroy et al., 2018). Very similar temperature values were recorded in both lagoons when growth patterns were different, so this parameter does not seem to be at the origin of the shift. Chlorophyll *a* can be used as a proxy for food for bivalves, but on a monthly scale no direct correlation was found between this parameter and shell growth patterns (Williams and Pilditch 1997; Babarro et al., 2003). We lack a high-resolution signal for chlorophyll *a*, which is likely to limits interpretations. However, data available in the literature underline the exceptional richness of the CSN lagoon, where chlorophyll *a* concentrations can exceed 10 $\mu g.L^{-1}$, superior to those of the SL (0.76 ± 0.25 $\mu g.L^{-1}$) or other Mediterranean ecosystems (Bec et al., 2011; Derolez et al., 2021). Therefore, the mussels living in CSN lagoon likely had low constraints on food availability. The detrimental conditions preventing the recovery of the mussel cage from October 2020 to January 2021, due to high turbidity and partial burial in sediment, could have led to a shift from mixed semidiurnal to daily increments during this period, initiated by lower feeding conditions and clogging of the gill system by excess of suspended matter (Peterson 1985). This is supported by the low CI values measured in January 2021. Thus, when *M. galloprovincialis* mussels are not under stressful trophic conditions, they appear to primarily deposit increments related to the local tidal regime (here mixed tides). In these environments, shell growth patterns alternate between mixed tidal, driven by the local tides, and daily when food conditions are limiting, controlled by biological clocks (Fig. 8C). It is unclear why mussels from lagoons do not follow the same pattern as

those from the sea, but rhythmic changes in the output of biological clocks have already been suggested for *M. galloprovincialis* (Bertolini et al., 2021). In the Venice lagoon, valve activity switches from tidal to bimodal (i.e. tidal and daily) periodicity over the year. As the main environmental parameters identified as possible zeitgebers of biological clocks (i.e. temperature and photoperiod) showed a large daily oscillation in these lagoons compared to the sea (Andrisoa et al., 2019; this study), the biological clock of mussels probably adopts a daily rhythm. Supernumerary increments might be generated when the biological clock and environmental cues are not synchronised (>2 increments. d^{-1}).

In the Mediterranean Sea, illustrated in this study by the bay of Banyuls-sur-Mer, mussels are exposed to a mixed tidal regime with a low range of water levels. Mussels form increments at a rate of ~1.7 increment.d^{-1}, in accordance with the local tidal regime. This growth pattern oscillates with semidiurnal tidal growth bands (~2 increments.d^{-1}), likely controlled by biological clocks when feeding conditions are limiting. Supernumerary growth bands (up to 3 increments.d^{-1}) may be formed when endogenous and environmental cues are not synchronised (Fig. 8D).

5. Conclusion

This study allowed a revision the rhythmic biomineralisation process of mussel shells, based on a combined molecular and sclerochronological approach using *M. galloprovincialis*. A short-term experiment showed that the deposition of growth increments is related to the activity of biomineralisation genes expressed in the basal bulb of the mantle, in the ventral margin of the shell. A long-term annual experiment using monthly chemical staining over one year revealed that growth patterns vary in space and time. In Mediterranean marine systems, shell increments are formed following a mixed semidiurnal tidal pattern, consistent with the local tidal regime. However, this pattern oscillates with tidal (at sea) or daily (in coastal Mediterranean lagoons) rhythms, likely controlled by biological clocks when conditions are less favourable for growth. Occasional supernumerary increments may be related to asynchronous environmental cues and biological clocks. These results provide a new overview of shell sclerochronology. However, the changes in the unit of time represented by growth increments are of paramount importance when considering the use of bivalve shells as biological archives, particularly in environments with low tidal range.

Funding

This project has received the financial support from the CNRS through the 80|Prime - MITI interdisciplinary program “TEMPO” and the MITI interdisciplinary program “ARCHIVE”.

CRediT authorship contribution statement

Victoria Louis: Writing – review & editing, Writing – original draft, Visualization, Software, Methodology, Investigation, Formal analysis, Data curation, Conceptualization. **Florian Desbordes:** Visualization, Investigation, Formal analysis. **Laurence Besseau:** Writing – review & editing, Validation, Supervision, Resources, Project administration, Methodology, Investigation, Funding acquisition, Formal analysis, Conceptualization. **Franck Lartaud:** Writing – review & editing, Validation, Supervision, Resources, Project administration, Methodology, Investigation, Funding acquisition, Formal analysis, Conceptualization.

Declaration of competing interest

The authors declare the following financial interests/personal relationships which may be considered as potential competing interests: Franck Lartaud and Laurence Besseau reports financial support was provided by Centre National de la Recherche Scientifique. If there are other authors, they declare that they have no known competing financial interests or personal relationships that could have appeared to influence the work reported in this paper.

Data availability

Data will be made available on request.

Acknowledgments

We acknowledge the “Conservatoire du littoral” of Perpignan, the “Syndicat mixte des bassins versants du Réart” and the “Syndicat Mixte RIVAGE” for allowing us to realize experiments in lagoons and the community from “Le domaine de Pedros” in Fitou that facilitated access to Salses-Leucate lagoon. We are grateful to Laurence Fonbonne (“Syndicat Mixte RIVAGE”), the “Pôle-relais lagunes méditerranéennes” and the FILMED network for sharing environmental data on lagoons and to the SOMLIT network for data at sea. We are thankful to captain Eric Martinez and the crew from the Néreis II as well as the divers, Jean-Claude Roca and Bruno Hesse (Sea Service from Oceanological Observatory of Banyuls) for the experiments at sea. We are also thankful to the “Réserve of Cerbère-Banyuls” for facilitating the work at sea. We acknowledge Eric Maria and Paul Labatut (from Banyuls Observation Sea Service – BOSS) for sea water sample processing. We are grateful to Erwan Peru for sharing temperatures beacons. We acknowledge the facilities of Biology platform of imaging (BioPIC). We are grateful to the Bio2Mar platform (http://bio2mar.obs-banyuls.fr) for providing access to instrumentation. We are very grateful to Stephane Hourdez who found back the ‘lost’ cage at Canet-Saint-Nazaire.

Appendix A. Supplementary data

Supplementary data to this article can be found online at https://doi.org/10.1016/j.marenvres.2024.106730.

References

Addadi, L., Joester, D., Nudelman, F., Weiner, S., 2006. Mollusk shell formation: a source of new concepts for understanding biomineralization processes. Chem. Eur J. 12, 980–987. https://doi.org/10.1002/chem.200500980.

Andrisoa, A., Lartaud, F., Rodellas, V., Neveu, I., 2019. Enhanced growth rates of the mediterranean mussel in a coastal lagoon driven by groundwater inflow. Front. Mar. Sci. 6, 753. https://doi.org/10.3389/fmars.2019.00753.

Arnaud, P., Raimbault, R., 1969. The Salses-Leucate pond. Its principal physicochemical characteristics and their variations (in 1955- 1956 and from 1960- 1968). Rev Trav Inst Pech Marit 33, 335–443.

Aschoff, J., 1981. Freerunning and entrained circadian rhythms. In: Biological Rhythms. Springer US, Boston, MA, pp. 81–93.

Babarro, J.M.F., Fernández-Reiriz, M.J., Labarta, U., 2003. In situ absorption efficiency processes for the cultured mussel Mytilus galloprovincialis in Ría de Arousa (northwest Spain). J. Mar. Biol. Assoc. U. K. 83, 1059–1064. https://doi.org/10.1017/S0025315403008270H.

Bargione, G., Vasapollo, C., Donato, F., Virgili, M., Petetta, A., Lucchetti, A., 2020. Age and growth of striped venus clam chamelea gallina (linnaeus, 1758) in the mid-western adriatic sea: a comparison of three laboratory techniques. Front. Mar. Sci. 7, 582703 https://doi.org/10.3389/fmars.2020.582703.

Bec, B., Collos, Y., Souchu, P., Vaquer, A., Lautier, J., Fiandrino, A., Benau, L., Orsoni, V., Laugier, T., 2011. Distribution of picophytoplankton and nanophytoplankton along an anthropogenic eutrophication gradient in French Mediterranean coastal lagoons. Aquat. Microb. Ecol. 63, 29–45. https://doi.org/10.3354/ame01480.

Benjamini, Y., Hochberg, Y., 2000. On the adaptive control of the false discovery rate in multiple testing with independent statistics. J. Educ. Behav. Stat. 25, 60–83. https://doi.org/10.3102/10769986025001060.

Bertolini, C., Rubinetti, S., Umgiesser, G., Witbaard, R., Bouma, T.J., Rubino, A., Pastres, R., 2021. How to cope in heterogeneous coastal environments: spatio-temporally endogenous circadian rhythm of valve gaping by mussels. Sci. Total Environ. 768, 145085 https://doi.org/10.1016/j.scitotenv.2021.145085.

Besseau, L., Benyassi, A., Møller, M., Coon, S.L., Weller, J.L., Boeuf, G., Klein, D.C., Falcón, J., 2006. Melatonin pathway: breaking the ‘high-at-night’ rule in trout retina. Exp. Eye Res. 82, 620–627. https://doi.org/10.1016/J.EXER.2005.08.025.

Buschbaum, C., Saier, B., 2001. Growth of the mussel Mytilus edulis L. in the Wadden Sea affected by tidal emergence and barnacle epibionts. J. Sea Res. 45, 27–36. https://doi.org/10.1016/S1385-1101(00)00061-7.

Carlucci, M., Krisciunas, A., Li, H., Gibas, P., Koncevicius, K., Petronis, A., Oh, G., 2020. DiscoRhythm: an easy-to-use web application and R package for discovering

rhythmicity. Bioinformatics 36, 1952–1954. https://doi.org/10.1093/BIOINFORMATICS.
Ceccherelli, V., Rossi, R., 1984. Settlement, growth and production of the mussel Mytilus galloprovincialis. Mar. Ecol. Prog. Ser. 16, 173–184. https://doi.org/10.3354/meps016173.
Checa, A.G., 2018. Physical and biological determinants of the fabrication of Molluscan shell microstructures. Front. Mar. Sci. 5, 353. https://doi.org/10.3389/fmars.2018.00353.
Cocquempot, L., Delacourt, C., Paillet, J., Riou, P., Aucan, J., Castelle, B., Charria, G., Claudet, J., Conan, P., Coppola, L., Hocdé, R., Planes, S., Raimbault, P., Savoye, N., Testut, L., Vuillemin, R., 2019. Coastal ocean and nearshore observation: a French case study. Front. Mar. Sci. 6, 324. https://doi.org/10.3389/fmars.2019.00324.
Comeau, L.A., Babarro, J.M.F., Longa, A., Padin, X.A., 2018. Valve-gaping behavior of raft-cultivated mussels in the Ría de Arousa, Spain. Aquac Reports 9, 68–73. https://doi.org/10.1016/J.AQREP.2017.12.005.
Connor, K.M., Gracey, A.Y., 2011. Circadian cycles are the dominant transcriptional rhythm in the intertidal mussel Mytilus californianus. Proc. Natl. Acad. Sci. U.S.A. 108, 16110–16115. https://doi.org/10.1073/pnas.1111076108.
Davenport, J., Chen, X., 1987. A comparison of methods for the assessment of condition in the mussel (Mytilus edulis L.). J. Molluscan Stud. 53, 293–297. https://doi.org/10.1093/mollus/53.3.293.
de Winter, N.J., Goderis, S., Van Malderen, S.J.M., Sinnesael, M., Vansteenberge, S., Snoeck, C., Belza, J., Vanhaecke, F., Claeys, P., 2020. Subdaily-scale chemical variability in a torreites sanchezi rudist shell: implications for rudist paleobiology and the cretaceous day-night cycle. Paleoceanogr. Paleoclimatol. 35, 1–21. https://doi.org/10.1029/2019PA003723.
de Winter, Killam, D., Fröhlich, L., de Nooijer, L., Boer, W., Schöne, B.R., et al., 2023. Ultradian rhythms in shell composition of photosymbiotic and non-photosymbiotic mollusks. Biogeosciences 20, 3027–3052. https://doi.org/10.5194/bg-20-3027-2023.
Derolez, V., Bec, B., Cimiterra, N., Foucault, E., Messiaen, G., Fiandrino, A., Malet, N., Munaron, D., Serais, O., Connes, C., Gautier, E., Hatey, E., Giraud, A., 2021. Obslag 2020 - volet eutrophisation.Lagunes méditerranéennes (période 2015-2020). Etat DCE de la colonne d'eau et du phytoplancton, tendance et variabilité des indicateurs. RST-LER/LR 21-16, 78p.
Dinno, A., 2017. dunn. Test: Dunn's Test of Multiple Comparisons Using Rank Sums.
Dunlap, J.C., 1999. Molecular bases for circadian clocks. Cell 96, 271–290. https://doi.org/10.1016/s0092-8674(00)80566-8.
Engel, J., 2017. Chapter 6: formation of mollusk shells. In: Engel, J. (Ed.), A Critical Survey of Biomineralization. Springer, pp. 29–40.
Fiandrino, A., Serais, O., Caillard, E., Munaron, D., Cimiterra, N., 2021. Bulletin de la Surveillance de la Qualité du Milieu Marin Littoral 2020. Région Occitanie - Départements des Pyrénées Orientales, de l'Aude, de l'Hérault, du Gard. Languedoc-Roussillon.
Fox, J., Weisberg, S., 2019. An R Companion to Applied Regression, Third. Sage, Thousand Oaks (CA).
Fuentes-Santos, I., Labarta, U., Fernández-Reiriz, J., 2018. Characterizing individual variability in mussel (Mytilus galloprovincialis) growth and testing its physiological drivers using Functional Data Analysis. PLoS One 13, e0205981. https://doi.org/10.1371/journal.pone.0205981.
Gao, P., Liao, Z., Wang, X., Bao, L., Fan, M., Li, X., Wu, C., Xia, S., 2015. Layer-by-Layer proteomic analysis of Mytilus galloprovincialis shell. PLoS One 10, e0133913. https://doi.org/10.1371/journal.pone.0133913.
Gerdol, M., Moreira, R., Cruz, F., Gómez-Garrido, J., Vlasova, A., Rosani, U., Venier, P., Naranjo-Ortiz, M.A., Murgarella, M., Greco, S., Balseiro, P., Corvelo, A., Frias, L., Gut, M., Gabaldón, T., Pallavicini, A., Canchaya, C., Novoa, B., Alioto, T.S., Posada, D., Figueras, A., 2020. Massive gene presence-absence variation shapes an open pan-genome in the Mediterranean mussel. Genome Biol. 21, 275. https://doi.org/10.1186/s13059-020-02180-3.
Hall, T., 2001. Biolign Alignment and Multiple Contig Editor.
Helm, B., Visser, M.E., Schwartz, W., Kronfeld-Schor, N., Gerkema, M., Piersma, T., Bloch, G., 2017. Two sides of a coin: ecological and chronobiological perspectives of timing in the wild. Philos Trans R Soc B Biol Sci 372, 20160246. https://doi.org/10.1098/RSTB.2016.0246.
Hervé, P., Bruslé, J., 1980. L'étang de Salses-Leucate, écologie générale et ichtyofaune. Vie Milieu 30, 275–283.
Hervé, P., Bruslé, J., 1981. L'étang de Canet-Saint-Nazaire (P.O.). Écologie générale et Ichthyofaune. Vie Milieu 31, 17–25.
Hüning, A.K., Melzner, F., Thomsen, J., Gutowska, M.A., Krämer, L., Frickenhaus, S., Rosenstiel, P., Pörtner, H.-O., Philipp, E.E.R., Lucassen, M., 2013. Impacts of seawater acidification on mantle gene expression patterns of the Baltic Sea blue mussel: implications for shell formation and energy metabolism. Mar. Biol. 160, 1845–1861. https://doi.org/10.1007/s00227-012-1930-9.
Karney, G.B., Butler, P.G., Speller, S., Scourse, J.D., Richardson, C.A., Schrder, M., Hughes, G.M., Czernuszka, J.T., Grovenor, C.R.M., 2012. Characterizing the microstructure of Arctica islandica shells using NanoSIMS and EBSD. G-cubed 13, Q04002. https://doi.org/10.1029/2011GC003961.
Komsta, L., 2011. Outliers: Tests for Outliers.
Langlet, D., Alunno-Bruscia, M., Rafélis, M., Renard, M., Roux, M., Schein, E., Buestel, D., 2006. Experimental and natural cathodoluminescence in the shell of Crassostrea gigas from Thau lagoon (France): ecological and environmental implications. Mar. Ecol. Prog. Ser. 317, 143–156. https://doi.org/10.3354/meps317143.
Louis, V., Besseau, L., Lartaud, F., 2022. Step in time : biomineralisation of bivalve's shell. Front. Mar. Sci. 9, 906085 https://doi.org/10.3389/fmars.2022.906085.
Lutz, R.A., Rhoads, D.C., 1977. Anaerobiosis and a theory of growth line formation. Science 198, 1222–1227. https://doi.org/10.1126/science.198.4323.1222.
Marie, B., Le, N., Zanella-Cléon, I., Becchi, M., Marin, F., 2011. Molecular evolution of mollusc shell proteins : insights from proteomic analysis of the edible mussel Mytilus. J. Mol. Evol. 531–546. https://doi.org/10.1007/s00239-011-9451-6.
Mat, A.M., Massabuau, J.C., Ciret, P., Tran, D., 2012. Evidence for a plastic dual circadian rhythm in the oyster Crassostrea gigas. Chronobiol. Int. 29, 857–867. https://doi.org/10.3109/07420528.2012.699126.
Mat, A.M., Charles, J., Ciret, P., Tran, D., 2014. Looking for the clock mechanism responsible for circatidal behavior in the oyster Crassostrea gigas. Mar. Biol. 161, 89–99. https://doi.org/10.1007/s00227-013-2317-2.
Miglioli, A., Dumollard, R., Balbi, T., Besnardeau, L., Canesi, L., 2019. Characterization of the main steps in first shell formation in Mytilus galloprovincialis: possible role of tyrosinase. Proc R Soc B Biol Sci 286, 20192043. https://doi.org/10.1098/rspb.2019.2043.
Mirzaei, M.R., Shau-Hwai, A.T., 2016. Assessing cockle shells (Anadara granosa) for reconstruction subdaily environmental parameters: implication for paleoclimate studies. Hist. Biol. 28, 896–906. https://doi.org/10.1080/08912963.2015.1052806.
Miyamoto, H., Miyashita, T., Okushima, M., Nakano, S., Morita, T., Matsushiro, A., 1996. A carbonic anhydrase from the nacreous layer in oyster pearls. Proc. Natl. Acad. Sci. USA 93, 9657–9660. https://doi.org/10.1073/PNAS.93.18.9657.
Miyamoto, H., Miyoshi, F., Kohno, J., 2005. The carbonic anhydrase domain protein nacrein is expressed in the epithelial cells of the mantle and acts as a negative regulator in calcification in the mollusc Pinctada fucata. Zool. Sci. (Tokyo) 22, 311–315. https://doi.org/10.2108/ZSJ.22.311.
Miyashita, T., 2002. Identical carbonic anhydrase contributes to nacreous or prismatic layer formation in Pinctada fucata (Mollusca : Bivalvia). Veliger 45, 250–255.
Miyashita, T., Hanashita, T., Toriyama, M., Takagi, R., Akashika, T., Higashikubo, N., 2008. Gene cloning and biochemical characterization of the BMP-2 of Pinctada fucata. Biosci. Biotechnol. Biochem. 72, 37–47. https://doi.org/10.1271/bbb.70302.
Miyazaki, Y., Usui, T., Kajikawa, A., Hishiyama, H., Matsuzawa, N., Nishida, T., MacHii, A., Samata, T., 2008. Daily oscillation of gene expression associated with nacreous layer formation. Front. Mater. Sci. China 2, 162–166. https://doi.org/10.1007/s11706-008-0027-3.
Moran, A.L., Marko, P.B., 2005. A simple technique for physical marking of larvae of marine bivalves. J. Shellfish Res. 24, 567–571. https://doi.org/10.2983/0730-8000(2005)24[567:ASTFPM]2.0.CO;2.
Mrosovsky, N., 1999. Masking: history, definitions, and measurement. Chronobiol. Int. 16, 415–429. https://doi.org/10.3109/07420529908998717.
NanoString Technologies Inc, 2017. Gene Expression Data Analysis Guidelines.
Nedoncelle, K., Lartaud, F., de Rafelis, M., Boulila, S., Le Bris, N., 2013. A new method for high-resolution bivalve growth rate studies in hydrothermal environments. Mar. Biol. 160, 1427–1439. https://doi.org/10.1007/s00227-013-2195-7.
Peharda, M., Black, B.A., Purroy, A., Mihanović, H., 2016. The bivalve Glycymeris pilosa as a multidecadal environmental archive for the Adriatic and Mediterranean Seas. Mar. Environ. Res. 119, 79–87. https://doi.org/10.1016/J.MARENVRES.2016.05.022.
Pérez-Ruzafa, A., Pérez-Ruzafa, I.M., Newton, A., Marcos, C., 2019. Chapter 15: coastal lagoons: environmental variability, ecosystem complexity, and goods and services uniformity. In: Wolanski, E., Day, J.W., Elliot, M., Ramachandran, R. (Eds.), Coasts and Estuaries: the Future. Elsevier, pp. 253–276.
Peterson, C.H., 1985. Patterns of lagoonal bivalve mortality after heavy sedimentation and their paleoecological significance. Paleobiology 11, 139–153.
Prieto, D., Markaide, P., Urrutxurtu, I., Navarro, E., Artigaud, S., Fleury, E., Ibarrola, I., Urrutia, M.B., 2019. Gill transcriptomic analysis in fast- and slow-growing individuals of Mytilus galloprovincialis. Aquaculture 511, 734242. https://doi.org/10.1016/j.aquaculture.2019.734242.
Purroy, A., Milano, S., Schöne, B.R., Thébault, J., Peharda, M., 2018. Drivers of shell growth of the bivalve, Callista chione (L. 1758) – combined environmental and biological factors. Mar. Environ. Res. 134, 138–149. https://doi.org/10.1016/J.MARENVRES.2018.01.011.
R Core Team, 2020. R: A Language and Environment for Statistical Computing.
Richardson, C.A., 1987. Tidal bands in the shell of the clam Tapes philippinarum (Adams & Reeve, 1850). Proc. Roy. Soc. Lond. B 230, 367–387. https://doi.org/10.1098/rspb.1987.0025.
Richardson, C.A., 1988. Exogenous and endogenous rhythms of band formation in the shell of the clam Tapes philippinarum (Adams et Reeve, 1850). J. Exp. Mar. Biol. Ecol. 122, 105–126. https://doi.org/10.1016/0022-0981(88)90179-7.
Richardson, C.A., 1989. An analysis of the microgrowth bands in the shell of the common mussel Mytilus edulis. J. Mar. Biol. Assoc. U. K. 69, 477–491. https://doi.org/10.1017/S0025315400029544.
Richardson, C.A., Crisp, D.J., Runham, N.W., 1980. An endogenous rhythm in shell deposition in Cerastoderma edule. J. Mar. Biol. Assoc. U. K. 60, 991–1004. https://doi.org/10.1017/S0025315400042041.
Roberts, E.M., Bowers, D.G., Davies, A.J., 2018. Tidal modulation of seabed light and its implications for benthic algae. Limnol. Oceanogr. 63, 91–106. https://doi.org/10.1002/lno.10616.
Rodríguez-Tovar, F.J., 2014. Orbital climate cycles in the fossil record: from semidiurnal to million-year biotic responses. Annu. Rev. Earth Planet Sci. 42, 69–102. https://doi.org/10.1146/annurev-earth-120412-145922.
Sano, Y., Okumura, T., Murakami-Sugihara, N., Tanaka, K., Kagoshima, T., Ishida, A., Hori, M., Snyder, G.T., Takahata, N., Shirai, K., 2021. Influence of normal tide and the Great Tsunami as recorded through hourly-resolution micro-analysis of a mussel shell. Sci. Rep. 11, 19874 https://doi.org/10.1038/s41598-021-99361-2.
Saurel, C., Gascoigne, J.C., Palmer, M.R., Kaiser, M.J., 2007. In situ mussel feeding behavior in relation to multiple environmental factors: regulation through food concentration and tidal conditions. Limnol. Oceanogr. 52, 1919–1929. https://doi.org/10.4319/lo.2007.52.5.1919.

Schöne, B.R., 2008. The curse of physiology — challenges and opportunities in the interpretation of geochemical data from mollusk shells. Geo Mar. Lett. 28, 269–285. https://doi.org/10.1007/s00367-008-0114-6.

Schöne, B.R., Pfeiffer, M., Pohlmann, T., Siegismund, F., 2005a. A seasonally resolved bottom-water temperature record for the period AD 1866-2002 based on shells of Arctica islandica (Mollusca, North Sea). Int. J. Climatol. 25, 947–962. https://doi.org/10.1002/joc.1174.

Schöne, B.R., Houk, S.D., Freyre Castro, A.D., Fiebig, J., Oshmann, W., Kröncke, I., Dreyer, W., Gosselck, F., 2005b. Daily growth rates in shells of arctica islandica: assessing sub-seasonal environmental controls on a long-lived bivalve mollusk. Palaios 20, 78–92. https://doi.org/10.2110/palo.2003.p03-101.

Schöne, B.R., Dunca, E., Fiebig, J., Pfeiffer, M., 2005c. Mutvei ' s solution : an ideal agent for resolving microgrowth structures of biogenic carbonates. Palaeogeogr. Palaeoclimatol. Palaeoecol. 228, 149–166. https://doi.org/10.1016/j.palaeo.2005.03.054.

SHOM, 2020. Horaires de marées gratuits du SHOM. https://maree.shom.fr/harbor/BANYULS/hlt/0?date=2020-06-24&utc=standard. (Accessed 13 September 2020).

Souchu, P., Bee, B., Smith, V.H., Laugier, T., Fiandrino, A., Benau, L., Orsoni, V., Collos, Y., Vaquer, A., 2010. Patterns in nutrient limitation and chlorophyll a along an anthropogenic eutrophication gradient in French Mediterranean coastal lagoons. Can. J. Fish. Aquat. Sci. 67, 743–753. https://doi.org/10.1139/F10-018/ASSET/IMAGES/F10-018E10H.GIF.

Strickland, J.D., Parsons, T.R., 1997. A practical handbook of seawater analysis. Bull. Fish. Res. Bd. Can, second ed.

Tanaka, K., Okaniwa, N., Miyaji, T., Murakami-Sugihara, N., Zhao, L., Tanabe, K., Schöne, B.R., Shirai, K., 2019. Microscale magnesium distribution in shell of the Mediterranean mussel Mytilus galloprovincialis: an example of multiple factors controlling Mg/Ca in biogenic calcite. Chem. Geol. 511, 521–532. https://doi.org/10.1016/j.chemgeo.2018.10.025.

Thaben, P.F., Westermark, P.O., 2014. Detecting rhythms in time series with rain. J. Biol. Rhythm. 29, 391–400. https://doi.org/10.1177/0748730414553029.

Tran, D., Perrigault, M., Ciret, P., Payton, L., 2020. Bivalve mollusc circadian clock genes can run at tidal frequency. Proc. R. Soc. A B 287, 20192440. https://doi.org/10.1098/rspb.2019.2440.

Treccani, L., Mann, K., Heinemann, F., Fritz, M., 2006. Perlwapin, an abalone nacre protein with three four-disulfide Core (whey acidic protein) domains, inhibits the growth of calcium carbonate crystals. Biophys. J. 91, 2601–2608. https://doi.org/10.1529/BIOPHYSJ.106.086108.

Trusevich, V.V., Kuz, K.A., Mishurov, V.Z., Zhuravsky, V.Y., Vyshkvarkova, E.V., 2021. Features of behavioral responses of the mediterranean mussel in its natural habitat of the black sea. Inl Water Biol 14, 10–19. https://doi.org/10.1134/S1995082921010132.

Venier, P., De Pittà, C., Bernante, F., Varotto, L., De Nardi, B., Bovo, G., Roch, P., Novoa, B., Figueras, A., Pallavicini, A., Lanfranchi, G., 2009. MytiBase: a knowledgebase of mussel (M. galloprovincialis) transcribed sequences. BMC Genom. 10, 72. https://doi.org/10.1186/1471-2164-10-72.

Warter, V., Erez, J., Müller, W., 2018. Environmental and physiological controls on daily trace element incorporation in Tridacna crocea from combined laboratory culturing and ultra-high resolution LA-ICP-MS analysis. Palaeogeogr. Palaeoclimatol. Palaeoecol. 496, 32–47. https://doi.org/10.1016/J.PALAEO.2017.12.038.

Williams, B.G., Pilditch, C.A., 1997. The entrainment of persistent tidal rhythmicity in a filter-feeding bivalve using cycles of food availability. J. Biol. Rhythm. 12, 173–181. https://doi.org/10.1177/074873049701200208.

Witbaard, R., Franken, R., Visser, B., 1998. Growth of juvenile Arctica islandica under experimental conditions. Helgol. Meeresunters. 51, 417–431. https://doi.org/10.1007/bf02908724.

Yan, H., Liu, C., An, Z., Yang, W., Yang, Y., Huang, P., Qiu, S., Zhou, P., Zhao, N., Fei, H., Ma, X., Shi, G., Dodson, J., Hao, J., Yu, K., Wei, G., Yang, Y., Jin, Z., Zhou, W., 2020. Extreme weather events recorded by daily to hourly resolution biogeochemical proxies of marine giant clam shells. Proc. Natl. Acad. Sci. 117,7038–7043. https://doi.org/10.1073/pnas.1916784117.

Zhao, M., Shi, Y., He, M., Huang, X., Wang, Q., 2016. PfSMAD4 plays a role in biomineralization and can transduce bone morphogenetic protein-2 signals in the pearl oyster Pinctada fucata. BMC Dev. Biol. 16, 9. https://doi.org/10.1186/s12861-016-0110-4.